



CISM COURSES AND LECTURES NO. 449
INTERNATIONAL CENTRE FOR MECHANICAL SCIENCES

PHASE CHANGE WITH CONVECTION: MODELLING AND VALIDATION

EDITED BY

TOMASZ A. KOWALEWSKI
DOMINIQUE GOBIN



Springer-Verlag Wien GmbH

CISM COURSES AND LECTURES

Series Editors:

The Rectors

Manuel Garcia Velarde - Madrid

Jean Salençon - Palaiseau

Wilhelm Schneider - Wien

The Secretary General

Bernhard Schrefler - Padua

Executive Editor

Carlo Tasso - Udine

The series presents lecture notes, monographs, edited works and proceedings in the field of Mechanics, Engineering, Computer Science and Applied Mathematics.

Purpose of the series is to make known in the international scientific and technical community results obtained in some of the activities organized by CISM, the International Centre for Mechanical Sciences.

INTERNATIONAL CENTRE FOR MECHANICAL SCIENCES

COURSES AND LECTURES - No. 449



PHASE CHANGE WITH CONVECTION:
MODELLING AND VALIDATION

EDITED BY

TOMASZ A. KOWALEWSKI
ACADEMY OF SCIENCES WARSAW

DOMINIQUE GOBIN
CAMPUS UNIVERSITAIRE ORSAY



Springer-Verlag Wien GmbH

The publication of this volume was co-sponsored and co-financed by the UNESCO Venice Office - Regional Bureau for Science in Europe (ROSTE) and its content corresponds to a CISM Advanced Course supported by the same UNESCO Regional Bureau.

This volume contains 135 illustrations

This work is subject to copyright.
All rights are reserved,
whether the whole or part of the material is concerned
specifically those of translation, reprinting, re-use of illustrations,
broadcasting, reproduction by photocopying machine
or similar means, and storage in data banks.

© 2004 by Springer-Verlag Wien
Originally published by Springer-Verlag Wien New York in 2004
SPIN 10984598

In order to make this volume available as economically and as rapidly as possible the authors' typescripts have been reproduced in their original forms. This method unfortunately has its typographical limitations but it is hoped that they in no way distract the reader.

ISBN 978-3-211-20891-5

ISBN 978-3-7091-2764-3 (eBook)

DOI 10.1007/978-3-7091-2764-3

PREFACE

Solid-liquid phase-change phenomena are present in a large number of industrial applications (materials processing, crystal growth, casting of metal – matrix composites, heat storage, food conservation, cryosurgery) and natural processes (iceberg evolution, magma chambers, crust formation). It is generally recognized that the dynamics of such phase change processes are largely influenced by natural convection. Numerical simulation of these non-linear, moving boundary, thermal and fluid flow problems is not a trivial task. The phenomena occurring during solidification of different materials or in different configurations are so diverse that no unique, simple description covering all ranges and scales is possible at the moment. Therefore, the modelling of phase change processes present in practical configurations requires the profound understanding of limitations of the existing physical and numerical models. Validation and verification of the numerical models before their implementation to practical industrial situations becomes an important issue if quantitative modelling of the real physical problems is a target.

The CISM course on Phase Change with Convection (PCC02) given in Udine in September 2002, followed PCC99 Workshop¹, which aimed to create a common platform for different groups working on modelling phase change problems. The main outcome of the workshop was to emphasize necessity for deeper understanding both the physical background and mathematical problems concerning modelling phase changes problems. The aim of the CISM course was to present a review of modelling phase change problems and of recent methods of numerical and experimental analysis used, with a particular focus on solidification coupled to convective flow. Special attention was given to the validation and verification of numerical codes and to the applications to practical problems.

The lecture notes prepared for the course are addressed to advanced students and scientists from engineering and applied sciences, as well as to physicists and mathematicians interested in the fundamentals of the field. There is large number of publications, workshops and reviews concerning modelling of solidification problems and only a minute fraction of these problems could be addressed during our short course. Nevertheless, we hope that theoretical background, discussion of physical phenomena, and practical examples of tailoring numerical codes given in our lectures will help readers to understand limitations of numerical models used for various engineering applications.

*Tomasz Kowalewski
Dominique Gobin*

¹ ESF Workshop on “Phase Change with Convection” held in Warsaw 1999, web page: <http://fluid.ippt.gov.pl/pcc99>

CONTENTS

Preface

| | |
|-----------------------------------------------------------------------------------------------------------------------------------------------|-----|
| Solidification Microstructure, Dendrites and Convection <i>by Gustav Amberg</i> | 1 |
| Microscopic-Macroscopic Modelling of Transport Phenomena During Solidification in Heterogeneous Systems <i>by Piotr Furmański</i> | 55 |
| Natural Convection at a Solid-Liquid Phase Change Interface <i>by Dominique Gobin</i> | 127 |
| Experimental Methods for Quantitative Analysis of Thermally Driven Flows <i>by Tomasz Kowalewski</i> | 171 |
| Modelling Methodologies for Convection-Diffusion Phase-Change Problems <i>by Fulvio Stella and Marilena Giorgi</i> | 219 |

Experimental Methods for Quantitative Analysis of Thermally Driven Flows

Tomasz A. Kowalewski

Department of Mechanics and Physics of Fluids, IPPT PAN, Polish Academy of Sciences
Warsaw, Poland

Abstract. Properly designed validation experiments are necessary to establish a satisfactory level of confidence in simulation algorithms. In this review recent achievements in the measurement techniques used for monitoring macroscopic flow field features are presented. In particular, optical and electro-optical methods, for example thermography, tomography or particle image velocimetry, are reviewed and their application to simple solidification experiments demonstrated. Computer supported experimentation combined with digital data recording and processing allows for the acquisition of a considerable amount of information on flow structures. This data can be used to establish experimental benchmarks for the validation of numerical models employed in solidification problems. Three experimental benchmarks based on water freezing in small containers are proposed to model flow configurations typically associated with crystal growth and mould-filling processes.

1 Introduction

1.1 Why do we need to measure?

Modern computational fluid dynamics (CFD) began with the arrival of computers in the early 1950s. The field of computational modelling of flow with heat and mass transfer has subsequently matured to the level it has. After half a century this is evidenced of a multitude of commercial codes purporting to solve almost every problem imaginable and suggesting the époque of expensive and complicated laboratory experimentation to have passed. Some foresights even profess construction of universal Navier-Stokes solvers, which implemented in a *black box* will be used in the predictable future almost the same way as pocket calculators now. Although all would welcome such a development, the validation of numerical results remains a concern tempering some of this optimism (Roache 1997). Typical difficulties in obtaining credible predictions for industrial problems lead to the often-encountered dilemma: Do we trust numerical simulations? This question seems especially pertinent when modelling solid-liquid phase change problems (see Gobin & Le Quere 2000), due to the complexity of the physical phenomena and the difficulties implied by the multi-scale nature.

One of the basic problems encountered by any model attempting to simulate physics involved in solidification is the broad diversity of length scales. The basic length scales fundamental to solidification processes arise from capillary forces, heat conduction, solutal diffusion, and convection. Different mechanisms of convection, including forced, natural, and Marangoni convection can all

contribute with a different strength. Hydrodynamic interactions with solid intrusions may lead to redistribution of species and local agglomeration. A wealth of flow patterns can result at the interface, e.g. cells, fingers and dendrites, depending on the parameters pertinent to the system. The complexity of the physical phenomena and the difficulties implied by its multi-scale nature create a plethora of non-dimensional parameters which attempt to merge these different scales into reasonable sets of equations.

In many cases coarse numerical results, resulting from simplified and idealised models, are accepted and successfully applied in engineering applications. A broad class of practical problems however exists, where knowledge of general flow behaviour alone is not sufficient to obtain a full quantitative elucidation of the phenomena. Examples include the distribution of fuel or soot in a combustion chamber, the transport of impurities in crystal growth and a considerable number of solidification problems, particularly where complex geometries and fluid compositions are concerned. The growing demand for high-quality alloys and semiconductors calls for means to predict and control the distribution of impurities and additives in grown crystals. Instabilities at the solid – liquid interface can lead to micro-segregation patterns in the deposition of impurities, which later may be detrimental to the material produced. Convective influence on cellular or dendritic growth remains an open topic for research. The interface grows in zones of instability; repeated branching results in a highly convoluted shape and topological changes may result. The behaviour of the intricate interface is very sensitive to boundary conditions applied to the interface and the flow field in its vicinity.

Strong nonlinearity of the governing equations combined with a moving boundary make *a priori* prediction of the consequences of inaccuracy or simplifications used in the numerical model almost impossible. The mechanism by which nonlinear phenomena induce reorganization of the flow patterns in unstable systems cannot be elucidated by small perturbation analyses. General methods to describe the above-mentioned phenomena in their highly nonlinear states are inevitably required. These regimes are obviously the most appealing to laboratory and computational experiments. Most industrial problems unfortunately involve configurations and substances, which are very difficult to investigate experimentally. Metals and metal alloys are opaque, their melting temperature is extremely high and their physical properties are not known precisely enough (Viskanta 1988, Incropera 1997). Hence, collected data is usually insufficiently accurate to provide a definitive answer on code reliability. One solution is to use so called *analog* fluids. These are transparent and have a low melting point. Such materials are most commonly aqueous solutions of salts, which crystallize with a dendritic morphology. Some organic liquids also lend themselves favourable to this purpose

It is evident that improvement in accuracy of both theoretical and numerical models and their validation using experimental data are imperative to solve such problems. Besides this very important task, there is still place for the *classical* laboratory experiment, enabling the discovery of new flow features based on *real life* observations. Solving complicated problems is easier when experimental feedback is present. For example, the simplification of thermal boundary conditions at apparently *passive* sidewalls was responsible for difficulties in numerical modelling of the flow structure in relatively simple cases of natural convection analysed in our laboratory. Only the use of *both* experimental *and* numerical methods allowed the fine structures of the thermal flow to be comprehensively understood. Difficulties in predicting changes in the flow pattern were triggered by a minor modification of the thermal conditions at traditionally idealised „passive” side walls. It

is impractical and usually impossible to include all possible factors when modelling the environment numerically. Properly planned experimental benchmarks alert one to the sensitivity of the flow to such conditions, which would otherwise be hard to predict. A brief review of experimental techniques for the study of heat and mass transfer flow problems is given with this objective in view in this work.

Velocity and temperature are the primary fields, which characterize a thermally driven flow. Point measurements were the preferred method to validate numerical codes in the past, however despite their high accuracy (e.g. Laser Doppler Anemometry), the limited number of simultaneously acquired values makes their use potentially questionable for the purpose of validation. It is therefore the author's opinion that 2-D or 3-D flow field acquisition methods are the only means, especially in the case of transient phenomena. One of this author's favourite 2D methods to determine both the temperature and velocity fields is based on a computational analysis of the colour and displacement of liquid crystal tracers. It combines Particle Image Thermometry (PIT) and Particle Image Velocimetry (PIV). Complete 2-D temperature and velocity fields were determined from two successive colour images taken at a selected cross-section through the flow. The 3-D flow structure can be reconstructed from a only few sequential measurements if the flow relaxation time is sufficiently long. In some cases even apparently good agreement of the measured and calculated fields does not guarantee their equivalence. Residual discrepancies may result in what are ultimately very different flow patterns and detection of these differences is a non-trivial task. Three-dimensional tracking of tracer particles suspended in the flow medium has been found to be particularly useful to this end. This is due to the strong sensitivity of the particle position to miniscule forces or numerical inaccuracy. It could be demonstrated that observed and simulated trajectories are often far from being in acceptable agreement, even for well known *standard* problems. In several cases simpler, 2-D particle tracking was found to be useful in demonstrating the basic differences between the observed and calculated flow patterns.

More generally speaking, we would also like to recover a complete, transient description of the analysed phenomena from the experiment. Only a very small fraction of the necessary data can, in reality, be extracted from the experiments to be compared with the numerical simulation. Quite often measurement of one of the parameters by a specific experimental method excludes simultaneous use of another method. Hence, planning the experiment must be preceded by an appropriate decision on the significance of collected data for a specific problem as well as a careful selection of the parameters to be monitored. One also has to remember the importance of an accurate description of initial and boundary conditions. Without this knowledge even the best numerical code can lead to an incorrect solution. Even a small deviation from the physical state ultimately causes the code to arrive at a different solution due to the non-linearity of the governing equations. Flow sensitivity to thermal boundary conditions defined at "passive walls", observed for simple convective flow was already mentioned. Problems with initial conditions are even more serious. Starting with an incorrect initial flow configuration (e.g. an incorrect initial temperature, velocity or concentration field) can ultimately result in differences in its behaviour, leading to different solutions. The usual practice of starting simulations from "*rest*" does not solve the problem. In the physical experiment there is always some uncontrollable motion and non-uniformity in the temperature, and concentration fields. Since these conditions are unpredictable, they cannot be used as initial conditions in the simulation. One option to minimize uncertainty is to force some

initial flow pattern and use it as an initial condition for the numerical and experimental runs. Such a method was implemented in our laboratory when resolving transient solidification problems.

The sources of the discrepancies between observed and numerical flow structures are plentiful. One of them is the three-dimensionality of the flow that complicates numerical modelling. Thermal boundary conditions (TBC) assumed at non-isothermal walls are in practice neither perfectly adiabatic, nor perfectly heat conducting, as is usually assumed in numerical models. The prevalent Boussinesq approximation for the physical determination of the fluid flow is not strictly valid for real fluids. In particular, viscosity dependence on temperature may generate severe discrepancies between expected and observed flow patterns in most liquids. In the work that follows we attempt to understand and explain the discrepancies between measured and calculated convective flow patterns in three instances of natural convection viz. a differentially heated cavity, a lid-cooled cavity and natural convection with a phase change (freezing of water). Finally, three simple configurations for the validation of numerical codes are proposed.

1.2 What do we need to measure?

Phase boundary. An accurate measurement of the shape and position of the phase front is of primary interest in solidification problems. Images of the solid/liquid interface are necessary for this purpose. This is an apparently simple task for transparent fluids, however detection of the interface for opaque substances needs application of specialized, and usually expensive tools. Measurements are usually of the form of digital images. Semi-automatic detection of the interface and the analysis thereof for comparison with numerical results can be significantly improved by use of image processing software. Image processing procedures considered basic here are smoothing, edge detection and the fitting of orthogonal functions to points at the interface.

Temperature. The description of transient temperature fields within the fluid, solidus and enclosure is the next most sought after goal of experimental modelling. Unfortunately, performing accurate temperature measurements is not an easy task. Point measurements (most common) usually give misleading information that can be. Differences, if present, erroneously can be interpreted as small changes of the flow structure close to the measuring point when compared with the numerical results. For the same reason agreement between numerical and experimental results can often be only superficial. Full field measurements, although not as accurate, may offer greater confidence.

Velocity. The fluid velocity field is important with regard to understanding both mould filling, as well as the complicated mass and heat transfer processes operative during solidification. Non-intrusive velocity measurements are non-trivial and measuring the velocity of a liquid metal flow is extremely challenging. Very few non-optical means are known for this purpose and even optical measurements are severely restricted. The full velocity field is still more challenging. The velocity vector has three spatial components and collecting complete three-dimensional information is both expensive and difficult. It is as a consequence of this that the flow field is usually reconstructed from two-dimensional cross-sections. Such methods, however much welcomed by those involved in numerical simulations, may lead to erroneous conclusions.

Concentration. Solutal convection is driven by species concentration gradients, yet another variable difficult to quantify experimentally. Serious discrepancies relating to the physical modelling of diffusion, the depletion of solutal by the solidus and the segregation of components in binary systems dog many numerical simulations. Some integral measurements of component concentration can be done using optical or electrical methods; however, the accuracy of such measurements is poor.

Material properties. Although it is not the intention of this paper to dwell on problems relating to the measurement of material properties, it is nonetheless worth noting that one of the difficulties in modelling industrial problems is the uncertainty in material properties. A “*comedy of errors*” is evident when comparing many published test cases in which material properties may differ from one another by an order of magnitude. Difficulties in getting data under extreme conditions of high temperature or pressure are often characteristic of many industrial problems. Hence, depending on the method used, collected data may differ substantially. One hopes to get more accurate measurements when using well known and documented *analog* fluids.

2 How do we want to measure?

In the pages to follow we describe a selection of experimental methods that can be useful for analysing thermally driven flow undergoing phase changes. Most of the described methods belong to the broad class of “*laboratory*” experimental methods, often precise and well defined, however, difficult to apply outside of the laboratory environment. Some of these methods are classical, well known standards. Some of them are rather *exotic*, and it is hoped that advancements in technology will make them more practical. Most of the full field measurements involve some kind of imaging procedure. Using optical methods, images of the flow are directly acquired. Non-optical methods such as ultrasound, X-ray, NMR, IR thermography, or tomography, convert acquired information to easily interpreted images. The images are stored as two or three-dimensional arrays in the computer memory and describe spatial or volumetric variation of a measured parameter. Using this format for the measured data it is easy to perform any basic image processing operation (see Bovik 2000, Jähne 1997). It can be used to smooth, to enhance or to extract details of the measured parameter. In the experimental methods presently to be described several image-processing operations are used to enhance information archived in the “images” of measured flow features.

2.1 Point measurements

Temperature measurements. Thermocouples and resistance temperature detectors (RTDs) are the traditional electric output devices used for measuring temperature, however, a number of semiconductor devices have recently been finding application at moderate temperatures (see Emrich 1981). Thermocouples are small sensors making use of the Seebeck effect, voltage existing at the junction of two different metals. The junction of two wires can be made extremely small and the resulting response time and spatial resolution of the thermocouple probe is therefore very good. Probes with a response time of several kHz and fractions of millimetre in size are commercially available. Very low voltage generated by thermocouples makes accurate measurement difficult, especially for low temperatures. Resistance thermometers (using Platinum wire with well-known properties) are more accurate and measuring a variation in temperature of the order of 0.001°C is

possible. One drawback of the resistance thermometers is their relatively large size (1 mm or more) and the response time of the probe is therefore in the order of seconds. Point measurements of temperature are very common in industrial experiments where the application of more sophisticated methods is inhibited. The intrusive nature of the methods makes point probes more useful in determining wall temperature and in the calibration of other methods, than in directly estimating the flow temperature field in laboratory experiments.

Very recently, ultrasound waves propagating in the fluid have been used to map the temperature field. One approach is based on the scattering of ultrasound from impurities in the fluid (Sielschott 1997). Another promising non-intrusive method, based on the variation of the speed of sound, has been proposed by Xu et al. (2002). The method can be used for opaque fluids, hence its application in industrial problems has revolutionary potential.

Velocity measurements. Only a few of the numerous techniques for measuring flow velocity are considered suitable for solidification problems in laboratory models. Some of these methods can be used directly or easily adopted for the bulk flow, while other more restrictive methods are useful for controlling external inflow. Monitoring flow velocity during industrial solidification is much more difficult.

Hotwire anemometry: Hot-wire and hot-film anemometry is a well-established velocity measuring method for fluids. It is based on the convective heat transfer from a small diameter heated wire, a function of the fluid velocity (see Goldstein 1983). In a hot-wire anemometer, the heat transfer assumed is that of a cooling cylinder perpendicular to the flow direction. Precise and fast measurement of the local fluid velocity is obtained by measuring the electrical power necessary to keep the temperature of the wire constant. A typical hot-wire probe has a 2-3 millimetres support with a short tungsten wire or film spanned between two metal electrodes. The dimension of the sensing wire can be as small as 1mm in length and several micrometers in diameter. It permits a frequency response as high as 100kHz. With additional wires (three-wire probe) it is possible to measure all three components of the local velocity field. Its relative simplicity and quick response make hot-wire anemometry one of the standard tools for studying turbulent flow. It is possible to achieve very accurate measurements of the local fluid velocity (relative error less than 1%). The main drawback of the method is sensitivity to impurities, which easily damage the very thin sensing wire. Hot-film anemometers, based on the same principle, are somewhat more robust. An insulating ceramic substrate is coated with a thin layer of metal (of the order of 5 micrometers). The sensing element is much larger in size but much more durable than that of hot-wire anemometer and it may be used in liquids.

Several instances in which hot-film anemometry has been used for investigating the thermally driven flow of liquids have been highly successful. With a modified probe it is even possible to obtain reasonable data close to the phase change front during solidification. The probe itself, however, creates serious perturbation of the investigated velocity field, as well as disturbing the local temperature field. It is less sensitive and accurate for low velocity flows. Its use for solidification experiments should therefore be limited to controlling global variables (e.g. inlet velocity) or to calibrate other measuring tools.

Laser Doppler Anemometry: The laser Doppler anemometer, also called a laser Doppler velocimeter (LDV), is a highly advanced non-intrusive method for measurements of fluid velocity. It is rather sophisticated and expensive, nonetheless, widely used in fluid mechanics research, includ-

ing turbulence measurements (Rinkevichius 1998). The method makes use of the well-known principle formulated by Christian Doppler, exploiting the fact that the motion of a radiating source relative to a detector results in a shift in frequency proportional to their relative velocity. The Doppler method of measuring local flow velocities is based on detecting the frequency shift of laser radiation scattered by particles moving within the flow. Since direct measurement of scattered radiation frequency in an optical range is often challenging, the method is adapted to measure instead, the frequency difference between the laser and scattered radiation. In particular, differential schemes with two crossing laser beams directed at a moving particle are widely used. The scattered radiation is recorded by a photodetector in some arbitrary position. The crossing point of the beams defines a measuring volume, typically 10^{-3}mm^3 , though this can be decreased by as much as three orders of magnitude. By applying additional phase shift it is possible to measure velocities from several $\mu\text{m/s}$ to high speed hypersonic flows. With two and three laser beams having different wavelengths the method can easily be extended to create a two or three component velocimeter. The laser Doppler anemometer is routinely used for detailed resolution of velocity fields. It is a non-intrusive and accurate method, well suited to a point diagnostic of the flow. There are, however, several drawbacks to the method:

- the method does not measure actual fluid velocity but the velocity of particles dispersed in the flow. Pure liquids therefore require some kind of seeding
- the method is sensitive to variation in refractive index and the optical properties of the light scattering particles. For complex fluids (mixtures and dispersions) variation of the composition and presence of a dispersed phase may produce a modulation of the detected frequency shift; the same effect is produced by local temperature variations.

Very careful analysis of the measured data is therefore necessary, especially for low velocity convective flow. The response time of the method is relatively short, however its sensitivity to optical variations of the analysed area makes it difficult to change location of the flow analysis quickly. Hence, a more detailed diagnosis of the flow field is practical only for steady state conditions. The method is expensive, especially for two or three component systems. Using the equipment requires a fair degree of operational competence and needs good optical access to the flow interior. In conclusion, LDA is an excellent and advanced method for non-intrusive flow diagnosis, however, its application in routine measurements of thermal convective flow with phase change is impaired tedious and possible only in limited instances.

Ultrasound anemometry: Ultrasonic devices use the same principle of Doppler effect to measure local flow velocity. A high-frequency acoustic pulse is directed at the flow interior, where it is reflected by particles or other acoustic discontinuities. Either the same device or a separate receiver receives the back-scattered acoustic wave. The distance travelled by the wave is simply related to the time for the pulse to travel from the transmitter to the receiver and to the speed of sound for the medium in question. By measuring the time taken for the echo to return, the source of the reflection signal can be localized. The Doppler frequency shift of the reflected signal carries information about flow velocity (see Takeda 1999). By repetition of the ultrasound pulses with continuously shifting time delay, a velocity profile along the beam direction is measured. For liquids, the transmitted carrier frequency may lie anywhere in the range of 0.5MHz to 10MHz, offering spatial resolution of 0.1 to 1mm and a velocity field measured with an error less than 5%. The pulsed Doppler ultrasonic velocity meters are commercially available as devices used to monitor flow of blood in arteries. Ultrasound Doppler anemometry, like LDA, is non-intrusive

method for measuring local fluid velocity; moreover it can automatically scan the flow along the direction of wave propagation. The method is consequently described as a “line-wise” method, and this description is particularly succinct in instances where the flow velocities are slow enough to neglect scanning time (typically about 1ms). The method does not require optical transparency of the flow medium and can therefore be used for opaque liquids. The method is, however, impaired by the acoustic properties of the walls and medium to be investigated. Uncertainties present due to the variation of the speed of sound with temperature and composition have to be accounted for to obtain accurate velocity data. At low flow velocities additional errors can be generated by dynamic interaction of acoustic waves with flow medium (particles), an effect usually called *acoustic streaming*. Ultrasound anemometry, nevertheless, seems to be an interesting alternative for penetrating solidifying flow fields of non-transparent media, e.g. metals. It is difficult to seed a molten metal, however it appears that acoustic waves may also interact with small heterogeneities in the fluid. Back-scattered ultrasound waves are used to determine both the scattering position and frequency shift. Successful tests have been performed using mercury, and more recently, liquid gallium (Brito et al. 2001). Preliminary tests with liquid sodium have also been performed. The experimental apparatus used by Brito et al. consists of a cylinder filled with liquid gallium, on the top of which is spinning disk. Particles 50 μm in diameter were used to seed the flow. An ultrasonic Doppler velocimeter with 8mm diameter transducer was used to measure the velocity profile of the fluid along the beam at various locations in the cylinder. The spatial resolution was about 6mm and the measured velocity had a standard deviation of 5-10%.

Concentration measurements. Solutal convection is very important to the acquisition of any observational data on variability in concentration. Point methods are usually simpler to use and some of these are discussed below.

Capacitance methods: The electric capacitance method for measuring components concentration is based on the principle that the dielectric constant of the fluid flowing between two external electrodes, depends on the concentration (Plaskowski et al 1994). This method of concentration measurement has attracted great interest because of its non-intrusive character and the simple interpretation. Accurate measurement of weak electrical signals produced at the sensor electrodes is, however, a non-trivial task. To achieve acceptable sensitivity to detect a phase boundary, the electrodes must have a surface of several square millimetres. Using several electrodes and sequentially measuring the potential between different pairs it is possible to collect data for tomographic reconstruction of the volumetric variation in concentration. Such a method was successfully applied for detecting phase boundaries, however its spatial resolution is still very low, about 5-10% of the characteristic distance between the electrodes.

Optical probes: The angle and intensity of reflected light depends on the change in refractive index of a medium. An optical probe consists of an optical fibre and photo-sensor. It measures the intensity of reflected light at an end, while immersed in a liquid. Optical probes are relatively accurate and useful devices for point sampling of a transparent fluid. They measure changes in refractive indices and can be used to determine local concentration in aqueous solutions of salts. If the temperature of the fluid changes, however, independent temperature measurement is necessary to correct additional change in refractive index. Some probes come ready equipped with a thermocouple for the simultaneous temperature measurement. The size of the probe may be as small as fractions of millimetre. Concentration changes in a flow are usually continuous and relatively

slow; hence response time is not an issue. The main drawback of this method is its optical basis; hence it can be applied only for transparent or semi-transparent liquids.

Electrical resistance methods: It is possible to ascertain temperature and concentration of dissolved phases by measuring electrical resistance between two electrodes, immersed in the test liquid. For solidifying liquids separate temperature information enables accurate determination of species concentrations. An accuracy of the method depends on both the size of the electrodes and the distance between them. The electrodes can be very small, of the order of millimetres or less. Conductivity of the liquid must be low in order to apply the method. It is therefore useful for aqueous solutions only, and not metals. The method can be extended to tomographic measurements if several electrodes are utilized. An example that employs such a system will be described in the section to follow.

2.2 Integral measurements

Schlieren, shadowgraphy and interferometry. These optical density measurement techniques are based on variations in the refractive index (see Mayinger & Feldmann 2001) and are very popular in aerodynamics. They have been used due to their simplicity and rapid response for many years in heat and mass transfer measurements. The sensitivity of the three optical methods are very different, the most sensitive being interferometry. This method is well suited to quantitative measurements. Hence, its use is more suited to the study of small density gradients; however, the well-tuned optics is necessary to avoid effects produced by windows and the external environment. The Schlieren and shadowgraph methods are more robust and less sensitive. It is important to note the following limitations of these techniques:

- they are essentially integral methods. They integrate the quantity measured over a length of the light beam. The information collected is a two-dimensional projection of the volumetric changes in the investigated area. These techniques cannot therefore resolve three-dimensional structures without additional information.

- they are sensitive to variation in the refractive index. Such changes are usually due to variable temperature and concentration. If both parameters change simultaneously, and this is certainly in the solidifying mixtures, an independent technique must be used to resolve the resulting ambiguity. Point or full field measurements of temperature/concentration are necessary, in addition, to evaluate concentration or temperature profiles.

The measuring technique of the Schlieren and shadowgraph technique is based on the deflection of a collimated light beam passing through a transparent medium with a variable refractive index. The shadowgraph is used to indicate the variation of the second derivative of the refractive index (normal to the light beam), which is responsible for deflecting part of the beam out of the plane of observation. The Schlieren uses optical focusing as the basis for a method strongly sensitive to rate of change in the gradient of the refractive index. A light source located at a focal point of a lens or concave mirror produces a parallel beam of light passing through the transparent medium under investigation. A second lens or mirror collects transmitted light and projects it onto the plane of observation. A diaphragm is located at the focal point of the second lens. The parallel light beam is focused on a small point at the opening of the diaphragm. Any variation of the refractive index in the media deflects light and is consequently screened by the edges of the diaphragm. Regions of light deflection show up darker at the plane of observation. Several different configurations for the Schlieren system exist. The optical arrangement in which a single mirror, double-pass system is

used, improves sensitivity of the method (Lehner et al 1999). Use of only one mirror is also an important cost saving factor, especially if illuminating large areas. In the classical Schlieren system a sharp plane (called a knife), which cuts only half of the beam, is used instead of a diaphragm. It allows for the detection of both orientation and direction of beam deflection. Hence, both the direction and orientation of the refractive index changes can be deduced from the intensity of the observed image. The human eye is not a good detector of light intensity; it is better at colour detection and variation of the Schlieren method, called colour Schlieren, has consequently been developed. It replaces the Schlieren edge with a set of transparent colour filters. The direction and magnitude of light deflection can be coded at the observation plane as a variation of colours by arranging a set of colour filters.

Interferometry is the preferred method in quantitative studies. Unlike the Schlieren and shadow-graph methods, an interferometer is not dependent on the deflection of a light beam (see Lehner et al 1999). To the contrary, any deflections of the beam in interferometry are undesirable, as they introduce errors. The underlying principle on which the method is based is the interaction of two light waves. One of two parallel beams is passed through the investigated volume of interest and the other is used as a reference beam. The phase shift induced by the variation of the refractive index in the first beam produces a variation in intensity in the region of their recombination. A camera, located behind the medium of interest, records the pattern of fringes of maximum and minimum intensity. The fringe pattern is directly related to the phase change, hence to the refractive index and consequently, density variation. By analysing the shape, density and the number of fringes produced by the interfering beams precise quantitative information on the variation in refractive index can be obtained (Van Buren & Viskanta 1980). A very narrow spectral width and coherence in the light source are crucial to interferometry. A laser light source is preferable, however, good results have also been reported using light emitting diodes (LEDs).

2.3 Full field direct measurements

Infrared Thermography. Infrared (IR) thermography is a two-dimensional, non-invasive technique for surface temperature measurement. IR thermography measures the long wave (thermal) radiation emitted by surfaces. *Black body* radiation increases with the fourth power of temperature and can be evaluated from a simple formula, the Stefan-Boltzmann law. General thermal radiation of the surroundings cannot be neglected and, in practice, the net measured radiation is given as a difference between the emitted and ambient radiation. Usually investigated surfaces have unknown emissivity, the extent to which a real body (surface) radiates energy compared to an ideal *black body*. Emissivity varies between 0 and 1 and must be known in order for the method to be applied. It makes quantitative measurements more difficult.

The modern infrared camera detects radiated electromagnetic energy in the infrared spectral range and converts it to an electronic video signal. This signal corresponds to a temperature map, which can be displayed or saved in the same way as an optical image. A properly calibrated infrared system allows for resolving temperature differences smaller than 0.1K in a response time of the order of $10^{-1} - 10^{-2} s$.

Infrared thermography, like any other optical method, requires transparency of the medium in order to be applied. Most standard materials and fluids are, however, opaque to infrared radiation. In such instances it is possible to investigate external thermal conditions, such as external wall or free surface temperature, only. It remains, nonetheless, a unique method for non-intrusive, full

field temperature measurement, useful in the control of thermal boundary conditions and in estimating heat fluxes (Carlomagno 1993). Prerequisites to temperature measurement by IR thermography are an accurate characterisation of the IR imaging system's performance, calibration of the IR camera, use of additional external optics to improve spatial resolution, determination of surface emissivity, identification of measured points and design of an optical access window composed of an appropriate material. Additional image processing techniques may be used to improve measurement accuracy.

Digital Holography. Holography is a natural extension of plane interferometry. Unlike classical interferometry, holography can store and reconstruct three-dimensional information. In the holographic interferometer, a reference and test light beam recombine on a camera plane to create a diffraction pattern. The test beam is created by a point source (pinhole) and it forms a spherical wave propagating through the volume under investigation. If both waves are coherent they form a very complex interference pattern when observed on the camera plane. The pattern usually consist of 1000 to 5000 fringes per millimetre, and recording therefore requires high resolution imaging systems, usually reliant on high quality photographic plates. The amplitude of the waves is stored as intensity variation. If the recorded plate is subsequently illuminated with coherent light source, the macroscopic pattern acts as a diffraction grating with variable constant. Observing the diffracted pattern from different directions facilitates the visualization of all optical details in the original medium. The main drawback of classical holography arises from problems in the digital recording of holograms. The spatial resolution of existing CCD cameras is still too low for quantitative holography. High-resolution films must therefore be used to obtain a sufficiently dense hologram, which can be used afterwards for quantitative measurements. The procedure is tedious, has limited potential for digital post-processing and is difficult to use for *online* flow analysis.

Digital holography is based on the same principle as holographic interferometry, the difference being that speckle images (a random interference pattern created by light scattered by a rough surface) are used. In holographic interferometry two object waves are recorded on a photographic plate and their interference pattern, called a hologram, is used. In digital holography the photographic plate is replaced by a video camera. The camera records the interference between an object wave and a reference wave as a *specklegram*, the relative angle being kept as small as possible so as to accommodate the low spatial resolution of the CCD sensors. The specklegram is a field of speckles whose size and intensity appears to vary randomly, however, the characteristics of the specklegram represent the characteristics of the object beam (see Fomin 1998). In digital speckle phase interferometry (DSPI), two specklegrams corresponding to two object waves are recorded separately in different frames on a CCD camera. An image processor can automatically calculate the difference between two frames during the acquisition of images. Combining two specklegrams gives rise to a speckle interferogram, the brightest fringes corresponding to the same phase shift (very much like in holographic interferometry). The most straightforward techniques for automatically measuring the phase shift from an interferogram are based on image intensity, i.e. on detecting fringe maxima and minima. Using these techniques for low-resolution CCD images produces sizable inaccuracies. One alternative is to change the phase during acquisition and collect a sequence of images. Such temporal phase shifting techniques can be done with a simple piezo driver mounted on the mirror. In this case, a known phase change is superimposed on the deformation phase between the two object waves. A different interferogram will be obtained for

each phase change. A deformation phase is now obtained for each CCD pixel by a simple equation involving the pixel intensity in several interferograms. A minimum of three interferograms is needed, however, four to five are usually used. The main advantage of these phase shifting techniques is that the processing is very simple and the precision is at least an order of magnitude better than that of the intensity based techniques. Fringe numbering is, furthermore, not a problem even in the most complicated interferograms. The possibility of correlating subsequent interferograms and calculating the relative phase shift due to fluid motion also exists. Such techniques allow for complete field measurement of the velocity field in the selected plane of flow (Andres et al. 1999) and are similar to particle image velocimetry.

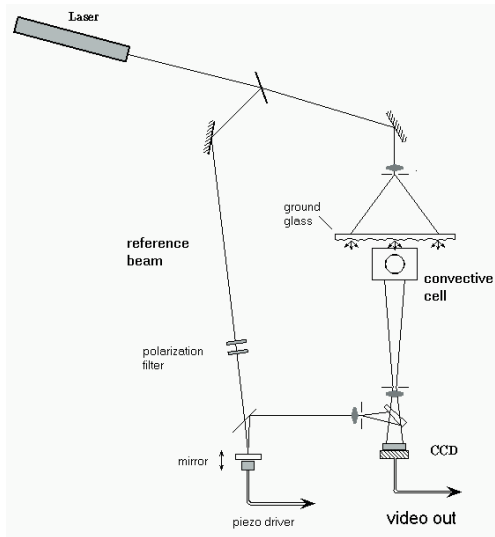


Figure 1. The DSPI arrangement used to investigate natural convection of water filled cylindrical cavity with cooled lid. A laser beam is split into a reference and illuminating beam. A piezo driver is used for the phase shift (Soeller 1994).

Attenuation methods. Light attenuation can be used to measure changes in the optical properties of a liquid. The principle on which this technique is based is the well-known exponential intensity attenuation law, which combines the absorption coefficient with properties of the subject medium. If all absorption parameters are known or the possibility for an accurate calibration procedure exists, the attenuation method allows the possibility of obtaining quantitative measurements of species concentration, during the solidification process. Optical changes arise due to natural differences in light absorption of binary mixtures or solutions. Dye is often added to one component to observe the convective flow associated with the solidification or melting. The pH indicator technique is very useful for introducing dye without disturbing a flow (McDonough & Faghri 1994). The technique involves a dilute solution of thymol blue and two electrodes located close to the region of interest. Applying voltage across the electrodes turns fluid in the vicinity of the positive electrode dark blue. The coloured fluid follows the flow perfectly as no difference in density

exists. The spatial distribution of the dye along a complex interface boundary may require the use of several light sources and cameras (Ibrahim et al. 2000).

For opaque liquids attenuation of short-wavelength radiation such as γ or X-ray absorption techniques are used. In these methods the attenuation coefficient is dependent on the third power of the atomic number. They are used to resolve the concentration field or even the motion of tracers in opaque solids and liquids. These methods have the advantage of being able to analyse *in situ* industrial solidification products. The attenuation method gives integral values across a projected volume in a manner similar to optical shadowgraphy. Single beam systems have a typical accuracy of 5-10% in measuring absorption values. Accurate determination of the concentration profile depends on the absorption properties of the investigated media and the calibration procedure.

Only the phase front is detectable in most practical applications of a single beam method. A more detailed evaluation of the concentration field requires many projections and tomographic reconstruction must be used to obtain a volumetric description of the absorption coefficient. Multi-beam systems are, however, complicated and expensive. Hence, their use for detailed laboratory analysis is very rare. Good results have been reported using attenuation methods with a collimated beam of neutrons on metals (Mishima & Hibiki 1996). Thermal neutrons can easily penetrate most metals, however they are strongly attenuated by such materials like hydrogen, water, boron, gadolinium, and cadmium. Kim and Prescott (1996) used of different capture cross-sections for neutrons to measure macro-segregation associated with solidification of a gallium-indium alloy.

Nuclear resonance and electro-magnetic tomography. Nuclear magnetic resonance can be used to detect liquid composition as well as the velocity within a volume. The spin-state magnetic resonance is created using a combination of a radio frequency and a permanent magnet field. The radio-frequency field is time gated and the delay time for a change in spin is used to measure both velocity and concentration. It is also possible to follow tracers immersed in a liquid with this method, obtaining images similar to those obtained using optical tomography. NMR devices are commercially available for medical purposes and are exorbitantly expensive. It is therefore likely that many advantages of this very attractive method remain as yet undiscovered to the science of fluid mechanics.

Novel developments in tomography offer an electro-magnetic flow measuring method, a promising new technique applicable to molten metals. The method is based on the analysis of eddy-currents induced by low frequency magnetic fields within the metallic melt (Pham et al. 1999). The induced current depends on the conductivity distribution. The eddy currents produce a scattered electro-magnetic field, which can be measured in the region exterior to the flow. The eddy currents are reasonably sensitive to continuous and discontinuous changes in the metal. They can be used to detect solidification front, mushy zone, and strong temperature or composition gradients. The technique is very advantageous for large-scale industrial problems, where generated eddy currents are strong enough for accurate measurements.

Resistance tomography. Electrical impedance tomography has become a promising method for the laboratory measurement of thermosolutal convection in recent years. The method is based on the measurement of current flowing between a working electrode and a reference electrode. Chemists often use the technique to measure the concentration of substances in solution. Analysis is complicated by effects such as chemical reactions at the electrodes, adsorption of reactants, elec-

tro-deposition and erosion of the electrode. The application of an alternating potential of appropriate frequency to the working electrode and the use of chemically inert electrodes is essential to all conductivity techniques. The method can be extended to volumetric measurements of the impedance distribution (concentration) within the solution. A multi-electrode system with alternative pairs of electrodes allows for the complete tomographic reconstruction of the conductivity field, hence, the concentration field is in this way resolved. Figure 2 shows the wiring in a 38mm Plexiglas cube used for studying the concentration of salt during the freezing process in a differentially heated cavity.

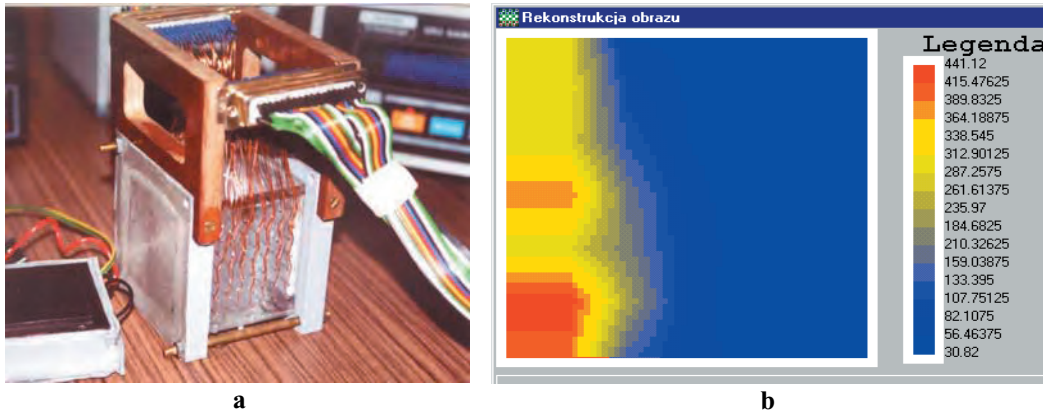


Figure 2. (a) The cavity used for concentration measurements. Two sets of 49 electrodes (7 rows x 7 columns) have been mounted on two opposite Plexiglas sidewalls of the cavity. Freezing of a salt water solution was investigated in the differentially heated cavity (Rucki et al. 2002). Ice created on the cold wall decreases electric conductivity of the investigated media. (b) The reconstructed resistance field for a salt water solution freezing from the left wall.

2.4 Tracer methods

Tracer methods are the most basic of all full field measurement techniques in fluid mechanics. Tracer methods are usually considered to be non-intrusive, however, it should be remembered that the principle involves the presence of seeding assumed neutral in the investigated fluid. Early visualization experiments based on the formation of a light sheet and tracer particles provided valuable quantitative information about the flow pattern and its basic properties. The rapid development of optical methods, lasers and finally digital imagery layered the foundation for the development of several new quantitative full field measuring techniques. For example Particle Tracking and Particle Image Velocimetry (see Grant 1994). Tracer methods arose from optical image analysis. Optical methods are usually inapplicable in most instances in volume solidification due to the opaqueness of the media e.g. metals and semiconductor crystals. However, it is noteworthy that the principles of quantitative flow image analysis are applicable to other than optical visualization methods, for example ultrasound, X-ray, NMR or infrared.

Flow Visualization using tracers. Flow visualization can be enhanced by addition of some small particles called tracers, whose paths within the flow provide basic information about flow struc-

ture. The tracers are selected on the basis of a compromise between their visibility and their ability to follow the flow. The quantitative interpretation of bulk flow observations is usually difficult. Hence, tracers are usually followed within some small “area of interest” by “cutting” the flow with a thin, well-defined plane of light (“light sheet”). Observing the plane from some angle, typically perpendicularly, only tracers within the light plane are visible. This basic visualization technique, called “light sheet” illumination, also happens to be the most convenient illumination method for particle tracking and velocimetry.

One of the biggest problems associated with flow visualization (and limitation of tracer methods) is the selection of a suitable seeding, the particles or inclusions responsible for detecting the fluid motion. A requirement of the seeding is that it has no motion relative to the fluid. This means that it has to be neutrally buoyant and its characteristic dimensions small enough to follow local flow acceleration. Using a simple models of hydrodynamic interactions, the limitation for particle diameter is dictated by $d^2 < 18\tau\mu / \rho_p$. Here τ , μ , ρ_p denote flow field relaxation time, viscosity, and particle density respectively. The buoyancy effects must be negligibly small thought sufficient to negate settling velocity, hence the particle diameter and fluid – particle density difference and must fulfil similar criterion, $V / d^2 \gg \Delta\rho g / 18\mu$, in which V is the local flow velocity component in the vertical direction. The dimension of particles of the seeding should, on the other hand, be large enough to be detectable by optical methods. In practice this means that the diameter should be larger than several micrometers. For very bright objects it is possible to record diffraction patterns using smaller particles (e.g. small air bubbles in liquid and fluorescent tracers). Seeding concentration is another issue and to avoid any effect on the flow pattern, concentration by volume must be very low (below 1%). This condition is usually easily satisfied, as high concentrations of the seeding are also counterproductive for recording methods. Ensuring the uniform concentration of tracers throughout the medium is a requirement not easily fulfilled. Residual particle – flow interactions usually cause redistribution; agglomeration in some regions and depletion in others. This can be highly problematic when dealing with complicated flow configurations and seeding may need to be done in very careful doses. The most commonly used seeding particles for liquids are latex or polystyrene spheres of a diameter between 1 and 50 micrometers. The use of thermochromic liquid crystals was found to be useful in experiments concerned with thermally driven flows. The typical diameter of such particles is between 20 and 50 micrometers, their density is close to that of water and they are easily visible when following the flow for typical thermal convection experiments.

Selection of a light source depends on the visualization technique to be used. For classical visualization volume illumination is sometimes used. Here diffused light from a standard light source is sufficient and bright particles are observed against a dark background. Backlight illumination using a parallel light beam is sometimes more convenient for particle tracking. Tracer particles are reproduced as black dots clearly visible on bright images and easy to identify by typical image processing software. Such illumination does, however, exclude multi-exposure of a single image, a technique very useful in digital recording.

Particle image velocimetry requires a well-defined plane of illumination, in which two or three components of the tracer velocity are evaluated. The quality of the light plane, i.e. uniform illumination intensity and small depth is an important deciding factor when it comes to the accuracy of the velocity evaluation. Lasers are commonly used to create light sheets because of their ability to emit monochromatic light with high energy density. Laser light can easily be bundled into a very

thin light sheet. Constant output lasers are common for flow visualization. The economic helium-neon (He-Ne) laser generating red light of a wavelength 633nm and power between 1 and 10mW can be useful for illuminating small flow fields. More powerful are argon-ion (Ar⁺) lasers which output green-blue light at wavelengths 514nm and 488nm and up to 100W. The intensity of light emitted by Ar⁺ lasers is high enough to illuminate large areas or to form short light pulses using electro-optical choppers. For better temporal resolution pulsed lasers are required, typically 10mJ to 1J per single pulse. The most widely used are ruby (Ru) and neodim (Nd:Yag) lasers. The first generates red light with wavelength of 694nm and can generate sequence of pulses over period of 1ms, the time duration of each pulse being of the order of about 30ns. The Nd:Yag lasers are available as tandems generating two 532nm wavelength light pulses within a time interval as short as 10ns. This facilitates the study of very fast flows in a large volume or micro-flows at considerably enlarged magnifications.

Monochromatic laser is an appropriate and easy solution for most visualization experiments, although there are cases where white light is required. One such case is the use of thermochromic liquid crystal tracers, where the colour of light refracted by TLC tracers indicates liquid temperature. A strong and relatively easily made light source is that produced by a linear halogen lamp with a tungsten filament spanning a 100-150mm tube. In our laboratory 1000W lamps with an additional air cooler and filament preheating circuit were used. High-energy xenon discharge lamps are employed for short illumination times. Such lamps consist of a 150mm long tube connected to a battery of condensers and can deliver as much as 1kJ of energy during a 1ms pulse. Repetition of the light pulses is relatively slow (several seconds). The total thermal load and condenser charging time are both factors limiting the repetition rate. In practice, two sets of condensers with an electronic switch can be used to allow two light pulses to be emitted from the same tube within approximately 200ms. The basic acquisition configuration in our laboratory is shown in Fig. 3.

The recording system is an important element in any tracer based measuring technique. Using a charged coupled device (CCD), an image can be stored directly in digital form, then numerically analysed. A typical CCD is a metal-oxide semiconductor composed of a two-dimensional array of closely spaced independent, light sensitive sensors, called pixels. The spatial resolution of the CCD recording is determined by the pixel dimension (usually 5 to 10 μ m) and the number of pixels in the sensor array. A standard CCD camera typically consists of a 768 x 572 pixel array, while high-resolution sensors may contain 5000 x 7000 pixels. By far the greatest handicap of CCD sensors is their refresh time i.e. image recording speed. This limitation is due to the charge read-out characteristics of the device. Increasing the transfer speed of photon-induced charges above a typical limit of 10 to 30Mpixels/s deprecates the signal quality, rapidly decreasing the signal to noise ratio. Hence, the frame rate of most commercially available cameras is limited to that of standard video i.e. 25 or 30 frame/s. Special CCD constructions that permit the acquisition of limited sequences of low-resolution images with frame rates up to 40000 images/s do, however, exist. In some applications, for example particle image velocimetry, two successive images are all that is necessary. Most standard CCDs fortunately have the ability to acquire two successive images within a very short time interval, a so-called straddle exposure. The first image is exposed on the CCD just before it is transferred to internal memory and the second one immediately after. Using the straddle exposure the time interval between both acquisitions can be as short as 200ns, but the next pair of images can be acquired after normal timing period.

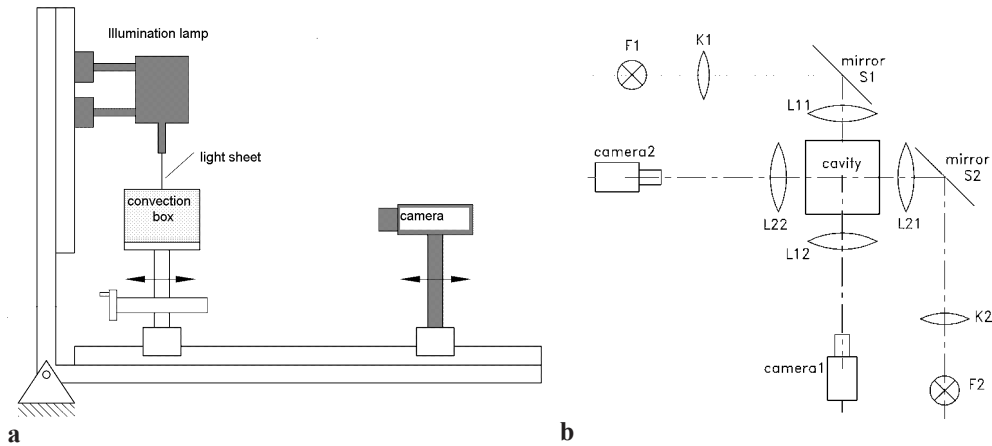


Figure 3. (a) - Acquisition system with CCD camera and light sheet illumination used for studying natural convection; (b) - two-camera system used for particle tracking in convective motion for a differentially heated, cube-shaped cavity

Electrical signals produced by each pixel of a CCD sensor are converted to a digital format and saved in the computer for future image analysis. The more professional CCD cameras, sometimes called digital CCD cameras, use an internal analogue-digital converter to provide a digital signal in 8 to 16 bit format, for monochrome images, and 24 bit format for signals containing RGB colours. The internal analogue-digital converter is matched to CCD characteristics so as to obtain optimum image quality. Special imaging boards (frame grabbers) are, however, necessary to acquire, display and archive such signals. Popular cameras, especially those having standard video format, deliver an interlaced analogue signal, which can easily be displayed on a television monitor. The analogue signal is acquired, then converted by a frame grabber to a digital format, before being stored and numerical processed. Quality of the digital image depends on the analogue-digital conversion procedure, and is impaired by low quality frame grabbers. Common causes of errors are conversion noise, conversion non-linearity and inaccurate timing (pixel position jitter). Another important property of the frame grabber is its ability to acquire images in real time (i.e. synchronic with the camera frame frequency) and to store them instantaneously to an on board memory or to a computer. The last solution is preferable as the computer memory (RAM) is easily expandable allowing an increasing number of images acquired. It is possible to transfer 1GB of data, with a speed well above 100MB/s, to memory (RAM) using current Pentium technology. This amounts to almost three hundred 16-bit, high-resolution images acquired at a rate of 30 frames/s. The image data must be transferred to the hard disk, before the next sequence can be acquired. The transfer process can take several minutes, and statistical analysis of the flow properties based on such images is therefore limited to relatively short (10s) bursts of data interrupted by save-to-disk time.

Particle Image Velocimetry. The basic concept and configuration of PIV is similar to that of a typical flow visualization (Raffel et al. 1998). The method is based on correlating parts of a sequence of flow images to establish their differences arising due to the flow movement. In contrast to the particle tracking method PIV does not search for single objects transported by the flow, instead it follows whole clusters of tracers, dyed regions within the flow, or changes in illumination. The PIV method assigns an average value to local flow velocity. Optical methods were used to correlate successive images, usually recorded on the same photographic plate (double exposure) in pioneering days of PIV. In recent times, pairs or short sequences of digital imagery, are numerically correlated by the computer to establish any local displacements caused by the motion of the flow, and this is sometimes specified by adding the adjective “digital” to the particle image velocimetry nomenclature (DPIV). The larger the amount of images in computer memory, the more detailed the study of transient flow behaviour becomes possible. It enables spatially resolved measurements of the instantaneous flow velocity in a minimal time and the detection of both large and small scale structures in the flow (Westerweel 1993). The use of PIV is very attractive in computational fluid dynamics (CFD), as the full field experimental data obtained in this way is more suitable to validating numerical simulations than the point measurements more commonly used in the past.

PIV evaluation requires two images, not necessarily two separate frames. Using single frame (double exposed) images the method can easily be adopted for high speed flows. The general trend is, nonetheless, to avoid the technical complications and ambiguity of single frame vector evaluations. In this work, we limit ourselves to PIV techniques based on pairs or longer sequences of images containing singly exposed images of the flow.

PIV analysis is based on the simple cross-correlation formula which can be stated as

$$R(x, y) = \sum_{i=0}^{M-1} \sum_{j=0}^{N-1} I_1(i, j) \cdot I_2(i+x, j+y)$$

for two arrays of pixels, where, the variables I_1 and I_2 are intensity values of the image arrays.

The whole image is divided into a regular mesh to sections, each demarcating a small interrogation area in a typical PIV evaluation procedure. Taking two small image arrays and manipulating the above summations we arrive to a cross-correlation function which describes the probability of matching the two arrays by means of an overlay. For each choice of sample shift, (x, y) , the sum of the product of all overlapping pixel intensities produces one cross-correlation value $R(x, y)$. The maximum of the correlation function corresponds to the statistically most probable shift to achieve a best match. This shift, or in terms of the flow displacement, gives the statistical local velocity vector when divided by known time interval between the two images. Clearly, it is necessary to run the cross-correlation operator over the whole image to obtain a full velocity field. It requires repeating the above summations and multiplications as much as a billion times per image, a computationally expensive procedure. An alternative procedure based on Fourier transforms is therefore more commonly used. Theoretical work on periodic signal analysis reveals that the cross-correlation of two signals is equivalent to the product a Fourier transform of the template signal with the complex conjugate Fourier transform of the correlated signal. Replacement of the correlation summations with Fourier transforms does not improve evaluation efficiency in itself,

however, Fourier transforms facilitate the use of Fast Fourier Transforms (FFT) giving rise to vastly more efficient algorithms. Instead of $O(N^2)$ computational operations the correlation process requires only $O[N \log_2 N]$ operations as a result of the introduction of fast Fourier transforms.

The FFT representation of the correlation function does have some drawbacks. The Fourier transform is an integral over an infinite domain and a discrete Fourier transform is, consequently, an infinite sum. Computing the transform over finite domains is justified only if the signal is periodic in all directions. Several methods are used to filter abrupt jump in the data from, artefacts arising from the use of finite image arrays. The application of Fourier transforms requires signals in the frequency domain; images of tracer particles produce a sequence of intensity peaks, which favour such analysis. The FFT gives much worse results when applied to images obtained from diffused visualization methods, like smoke, dye or intensity fluctuations. In such cases classical cross-correlation or other, similar image processing methods are more appropriate (Quenot et al. 1998, Gui & Merzkirch 1996, 2000).

Another drawback of standard PIV analysis has its origins in the interrogation window, i.e. in the principle of evaluating a cross-correlation function for a fixed sub-array of the full image. A full vector field is obtained by the use a moving step-by-step interrogation window across the whole image. Correct dimension assigned for this sub-array is crucial for the accuracy and dynamics of the evaluated velocity field (Westerweel et al. 1997). Although the spatial resolution increases with a diminished interrogation window, its minimum size is limited by two factors. Firstly, a sufficient number of tracers must be present in the interrogation window, otherwise the FFT based procedure fails to work properly due to poor statistics. Therefore, only windows larger than 16x16 pixels are used in practice. Secondly, the dimension of the interrogation window limits the maximum detectable displacement. Displacements only smaller than about half the window size can be detected. Hence, large windows are advisable for the velocity measurements when the dynamics has to be increased. Finding a compromise is not possible without some additional procedure. If the flow is relatively slow, a simple solution is to take short sequences of images acquired at suitably selected intervals. The cross-correlation analysis performed between different images of the sequence allows to preserve the accuracy for both the low and high velocity flow regions. Post-processing is necessary to combine the sequence of flow fields with the one with improved parameters. Hart (1998) proposed another solution. In this approach high-resolution analysis is achieved by the iterative use of local correlation results. The interrogation area is divided into smaller areas after standard, large window PIV correlation analysis, and each subdivided region is re-interrogated in the same manner, except that the second window is shifted by a displacement determined by the previous correlation (offset). Subdivision and re-interrogation is repeated until the size of the interrogation area attains a minimum (can be as small as the size of the individual particle-image size). The method works fine for smooth velocity fields. However, large velocity gradients lead to a false estimation of the initial window offset and subsequent evaluations with smaller windows completely degrade the vector field in this region.

Pre-processing and post-processing plays an important role for PIV as images are often less than ideal. They contain noise arising from the acquisition procedure, illumination in the image plane is never perfectly uniform, both wall reflections and the scattering properties of the seeding vary according to the illumination angle. Sever intensity differences between light pulses are also frequent when using laser or flash lamp illumination. These effects all can ruin PIV evaluation procedure and FFT based evaluation is particularly sensitive to image quality. Various image

processing methods can be used to improve contrast and achieve uniform illumination by automatically analysing intensity histograms for each image of the correlated sequence and modifying them accordingly. Using direct cross-correlation (or a similar algebraic method), the adjustment of the intensity of each subsection effectively removes non-uniformity in the illumination of the image. A good contrast of images of the tracers is important for FFT based evaluation. To improve their visibility contour detection filters are sometimes used. Experience, nonetheless, shows that such procedures can sometimes result inversely. It is author's experience that the use of local thresholding filter favourable enhances PIV images, allowing for the extraction of particle images from non-uniformly illuminated backgrounds. The resulting images have almost uniform intensity, particles' shape is clearer and the bright areas which may be attributed to reflections are filtered out.

Identification and precise evaluation of the correlation peak location is crucial to the PIV process. The correlation values exist only for integral shifts since image data is discretised. By using interpolated intensity values and simply doubling the size of the analysed interrogation array, the accuracy of the evaluation improves to 0.5pixel . Irregular peak shapes with a double or triple hump form are frequently observed due to non-ideal processing conditions and a simple search for the maximum value may lead to large errors. A variety of methods for improving the estimation of the correlation peak location have been proposed. A simple and robust method to find location of the peak maximum is to fit the correlation data to some function. Parabolic peak approximation is by far the simplest and fastest procedure. The best fitting paraboloid is obtained by taking the peak value, and four or eight adjoining values of the correlation function. A Gaussian peak fit is slightly more accurate but also more tedious. Since peak approximation methods use more than one point in evaluating the peak shape, there is statistical improvement in the estimation of the peak location involving fractions of a pixel. The best values reported in the literature for the spatial resolution are close to 0.1 pixel .

PIV processing results usually need additional post processing. Correlation based PIV evaluation inevitable leads to spurious vectors due to its statistical character and the detection of spurious vectors involves a variety of approaches, or combination thereof. Some indications of the quality of the vector results can be obtained by analysing the correlation function. The detection of odd behaviour in the correlation function in some regions can lead one to critically evaluate certain vectors, either removing or interpolating them. A variety of interpolation techniques can be applied to smooth the PIV velocity field, most of them are already well-known to image processing. An adaptive procedure must normally be used as the number of spurious vectors can vary depending on the locality. It selects the degree of interpolation according to the number of removed vectors and additional constrains supplied (e.g. maximum gradients, maximum velocity). A simple median filter or two-dimensional smoothing interpolation can be applied locally and used to remove points deviating in excess of some predefined threshold, based on the assumption of a smooth velocity field. In instances where the proportion of removed vectors is high, values of the surrounding vectors can bias the interpolation and lead to false results. It is useful therefore to include some additional information pertaining to the vector field, if such information is known. If the flow can, for example, be assumed to be two-dimensional, the evaluated vector field must satisfy the continuity equation. The velocity at the walls bounding the flow field should diminish asymptotically.

Three-dimensional velocity field measurements. Fluid flow is, generally speaking, always three-dimensional. It is, nevertheless, common to analyse two-dimensional projections due to the limitation imposed both numerically and experimentally. In many cases the out-of-plane velocity component cannot, however, be neglected as it plays an important role in both overall mass and heat transfer. Real time three-dimensional velocity measurements are non-elementary. Holographic PIV could probably be deemed the most promising method for the recovery of full volumetric information about tracer locations in the flow using a single illumination shot. But development of holographic PIV is still at an infant stage and the apparatus is complicated and difficult to arrange. The stereo-PIV technique is much simpler and available commercially. It employs two standard PIV cameras to observe the flow in a illuminated plane. The third component of tracers' motion can be recovered using parallax (Raffel et al. 1998). It should be stressed, nevertheless, that the three-dimensional information gathered in this way still only pertains to the cross-section of the flow in the illuminating light sheet. A full description of the flow requires multi-plane illumination.

It is possible to make use of tomographic methods which employ ultrasound sensors, or magnetic resonance (NMR) to resolve three-dimensional flows. The accuracy of results unfortunately does not justify the effort and costs of the techniques.

Particle tracking methods are usually three-dimensional if more than one camera is used. Three-dimensional particle tracks are consequently reconstructed and the three-components of the tracer velocity evaluated (Englemann et al. 1998). Typical limitations of the method arising from particle density give rise to a very sparse velocity field. Particles also due to hydrodynamic interactions prefer some regions of the flow, whereas others are rarely visited. From statistical point of view such a description of the flow is strongly biased (Yarin et al. 1996).

Figure 3b gives an example of experimental arrangement for three-dimensional particle tracking. It employs two cameras oriented perpendicularly through the investigated cavity (Bartels-Lehnhoff 1991, Hiller et al. 1992, Mitgau et al. 1994). Bright field illumination is used with help of two light-emitting diodes. Tracers are visible in each pair of images as black dots on a white background. Evaluation of the tracers' position can be simplified by automatic subtraction of the "zero" image (the image without particles). Any non-homogeneities arising from the optical channel are automatically removed in this manner and only moving objects are detected.

Although three-dimensional data acquisition is challenging, most of the two-dimensional methods using a light sheet can be relatively easily adapted to obtain volumetric information, providing the flow relaxation time is sufficient. This is accomplished by scanning the flow area with a moving light sheet. In practice, a system of rotating mirrors or mechanical shift of the analysed enclosure is used. The method is the simplest to use in the case of relatively slow natural convection or solidification (typical for the laboratory scale experiments), and has been successfully applied in experiments on natural convection during the freezing of water (Kowalewski & Cybulski 1996, 1997).

Liquid Crystals Thermography. Liquid crystals are highly anisotropic fluids, existing between the boundaries of the solid and the conventional, isotropic liquid phase. Liquid crystals temperature visualisation is based on the refraction of particular colours (light wavelengths) at specific temperatures and viewing angle by some cholesteric and chiral-nematic liquid crystal materials (Straley 1994). Normally clear, or slightly milky in appearance, thermochromic liquid crystals

appear to change their colour to red in response to increase of temperature, followed by yellow, green, blue, violet, finally turning colourless again at higher temperatures. In this way liquid crystals used as temperature indicators modify incident white light and display colour of a wavelength which can be associated to temperature. Thermochromic liquid crystals can be painted on a surface (Hai & Hollingsworth et al. 1996, Sabatino et al. 2000, Preisner et al. 2001) or suspended in the fluid to render the temperature distribution visible (Hiller & Kowalewski 1987, Dabiri & Gharib 1991). Application of TLC tracers facilitates instantaneous temperature and velocity fields measurements in a two-dimensional cross-section of the flow. It is a unique method of combining full field temperature and velocity measurements. The colour is red at the low temperature margin of the colour-play interval and blue at the high end. The particular colour-temperature interval depends on TLC composition. It can be selected for intervals of about 0.5°C to 20°C and associated with temperatures of -30°C to above 100°C . These colour changes are reversible providing the TLCs are not physically or chemically damaged. They can consequently be accurately calibrated and used as precision indicators of temperature. The colour play range must obviously be selected to match the temperature variation of the problem in question. Pure liquid crystal materials are thick, greasy liquids, which are difficult to handle under conventional heat transfer laboratory conditions. TLCs are also sensitive to mechanical stress. A micro-encapsulation process, enclosing small quantities of liquid crystal material in transparent, polymeric capsules, was developed to solve problems with sensitivity to stress and chemical deterioration.

In the past liquid crystals have been extensively applied in the qualitative visualisation of entire, either steady state, or transient temperature fields on solid surfaces. Since quantifying colour is a difficult and somewhat ambiguous task, application of thermochromic liquid crystals was initially largely qualitative. Application of the colour films or interference filters was tedious and inaccurate. Quantitative and fast temperature measurements were only brought about with the adoption of the CCD colour camera and digital image processing. The rapid development of hardware and software image processing techniques has made the use of inexpensive systems, capable of real-time, transient, full field temperature measurements using TLCs possible (Hiller et al. 1990, 1993, Koch 1993, Park et al. 2001). By disseminating the liquid crystal material throughout the flow, TLCs become not only classical tracers for flow visualisation, but simultaneously, minute thermometers monitoring local fluid temperature. The typical diameter of TLC tracers is $50\mu\text{m}$. With the density close to that of water, TLC tracers are well conveyed in liquid flows. The response time of the TLC material is between 3 and 10ms, sufficiently fast for most typical thermal problems in fluids. A collimated white light source is required to illuminate selected cross-sections of the flow (light sheet technique) and colour images are acquired by a camera oriented perpendicular to it.

While tracer colour is intended to indicate temperature distribution of the liquid, the observed colour can also depend on the angle of observation. The author's investigations have shown that this relation is linear with a 10° change of angle being equivalent to a 0.07°C change in temperature (Hiller et al. 1988). It is therefore vitally important that the angle between the illuminated plane (light sheet plane) and the camera is fixed and the viewing angle of the lens is small. In a typical experiment, the flow is observed at 90° using a 50mm lens and a $1/3'$ sensor (i.e. the camera-viewing angle was smaller than 4°).

Temperature measurements using TLC are based on the colour analysis of images and needs a appropriate calibration. The best measure of colour would be a spectral analysis of refracted light.

In earlier investigations, sets of interferometric filters were applied to analyse the variation in light intensity, recorded by black & white video camera. The development of digital imagery has led to the acquisitions of ready pre-processed information by colour video camera. Colour video cameras split light into three basic colours components: red, green and blue (RGB). This process is known as trichromatic decomposition. Each of the three colour components is usually recorded as a separate 8-bit intensity image. Numerous methods of subtracting colour information from a trichromatic RGB signal exist. The most straightforward is to convert the RGB trichromatic decomposition to another trichromatic decomposition based on hue (colour value), saturation and intensity (HSI). Such decomposition is extremely common in image analysis and also serves as a natural means of converting colour images to their black & white representation. Classical conversion of a RGB colour space to an HSI decomposition is based on three simple relations. Light intensity (or brightness) is defined as the sum of its three primary components. The saturation represents colour purity, i.e. the relative value of the remainder after subtracting the amount of colourless (white) light. The hue relates to the dominant colour and is usually obtained from the algebraic or trigonometric relation between the two dominant primary colours. Temperature is determined by relating hue to a temperature calibration function. This is the most critical stage of TLC based thermography. Light refracted by TLC is not monochromatic, even if the observed sample has a uniform temperature. Colour depends on observation angle, scattering properties of the tracers, the colour and refractive index of the liquid and may also vary with the size of the tracers. Additional factors, like the colour of the light source, the colour transmission properties of the acquisition system, as well as reflected and ambient light. The observed colour may also depend on light intensity. Very careful calibration is therefore necessary to obtain quantitative information. The calibration procedure is performed with an identical experimental arrangement to that used for measurements. The difference is that the bulk temperature of the liquid containing the suspended tracers must be extremely uniform and well defined. This is achieved by keeping the experimental cell at a constant temperature and continuously mixing the liquid with a magnetic stirrer. The cell temperature is gradually adjusted by small increments (usually with 0.3°C steps), and several sequences of images are acquired for future processing. An area of about 50 x 50 pixels in the vicinity to the temperature sensor is extracted from each image. Hue evaluation is performed for each pixel, under constraints of minimum and maximum pixel intensity and minimum saturation. "Good" pixels are used to build a hue matrix, which is smoothed using a 5x5 median followed by a low pass filter. An average hue value is then calculated for each image and used as a reference point for the calibration procedure. The procedure is repeated for several images over the TLC's full colour range. It is accomplished by fitting polynomial with variable degree. Outliers are removed from a preliminary fit to obtain a smooth temperature-hue function. The accuracy of the measured temperature depends on the colour (hue) value as a direct consequence of the non-linearity of the curve. The relative error varies from 3% to 10%, and is based on the temperature range defined by the TLCs colour-play limits. For the TLCs used in our experiments (TM Merck), an absolute accuracy of 0.15°C results for low temperatures (red-green colour range) and 0.5°C for high temperatures (blue colour range). The most sensitive colour region is the transition from red to green, which occurs over a temperature change less than one degree Celsius. The same experiment can be repeated using different types of TLCs to improve the accuracy of temperature measurements. The combined measurements cover an extended temperature range, although the method is tedious and requires easy repetition of the experiment.

The application of TLCs to phase change problems bears additional experimental constraints. The phase change temperature must be well defined within the investigated temperature range. Hence, a proper selection of the TLC material becomes crucial. In addition, the solidus surface produces strong light scattering and reflections., which can generate unexpected colour shifts, image distortions in regions adjacent to the phase front. These must all be accounted in the calibration procedure.

In addition to being temperature indicators, TLC tracers are well suited to a seeding role in any visualization experiment, particularly particle image velocimetry. Typical PIV images, correlation-ready, are obtained by converting the colour images to intensity component and applying the usual contrast enhancement procedure. An additional advantage of TLCs is their almost complete transparency to diffused light. Hence, it is much easier to observe particles deep within the flow. Their major drawback is that the intensity of scattered light strongly decreases in regions where local fluid temperature is out of the TLCs colour variation range.

3. Examples of investigated problems

3.1 Particle tracking

Particle tracking is a extremely useful in validating computer simulations of flow. While numerically generated streamlines allow detailed analysis of flow structures, comparison with observed particle tracks provides the most reliable code verification. Some examples of the application of a particle tracking system to natural convection studies are shown below. Several images were recorded at intervals and added to the computer memory to obtain a general view of the flow pattern. The resulting images are similar to multiple exposures, showing both the flow direction as well as its structure. Only a limited number of two-dimensional projections of the particle tracks can be acquired in this way. Better elucidation of three-dimensional flow structures is possible using a stereoscopic observation of the particle paths.

A special procedure has been developed for this purpose, which allows the detection and automatic tracking of particles suspended in the flow medium. Two CCD cameras, each integrated with an identical frame grabber installed in a single personal computer, capture the images. A few, almost nearly neutrally buoyant tracers of a diameter of about $150\mu\text{m}$ are observed against a bright background from two perpendicular directions. The identification of particles followed by automatic data evaluation and storage enabled experiments to continue unattended over periods as long as several days.

Effect of thermal boundary conditions. The general approach to thermal boundary conditions (*TBC*) imposed on the limiting boundaries of a computational domain is very pragmatic. Idealizations like adiabatic, isothermal or imposed heat flux are widely accepted due to inevitable lack of detailed information. It is certainly not efficient to extend the solution domain to calculate all effects of the surrounding environment on the investigated flow. This would entail unnecessary complication. In fact some heat transfer problems appear not to suffer from *TBC* model simplifications, but it seems worth to sum up some of the possible consequences.

Our observations suggest that *TBC* imposed at the non-isothermal walls may effectively modify the three-dimensional flow structure (Hiller et al. 1990). The main flow pattern in the differentially heated cavity is predictable for most investigated case, and can be calculated by way of simple *2-D*

modelling of the symmetry plane. The 3-D modelling does, however, become more sensitive to *TBC*, away from the symmetry plane. A good example of these *TBC* effects can be found in the standard „double glazing” problem for a cube-shaped cavity. The flow pattern at the symmetry plane has one or two vortex-like rings, transporting fluid back and forth between isothermal walls. This flow is crucial to the overall heat transfer, is predictable and rather insensitive to *TBC* at the thermally passive walls. The 3-D flow structure consists in one or two spiralling motions, responsible for cross-flow from front and back walls to the cavity centre, in addition to the main recirculation.

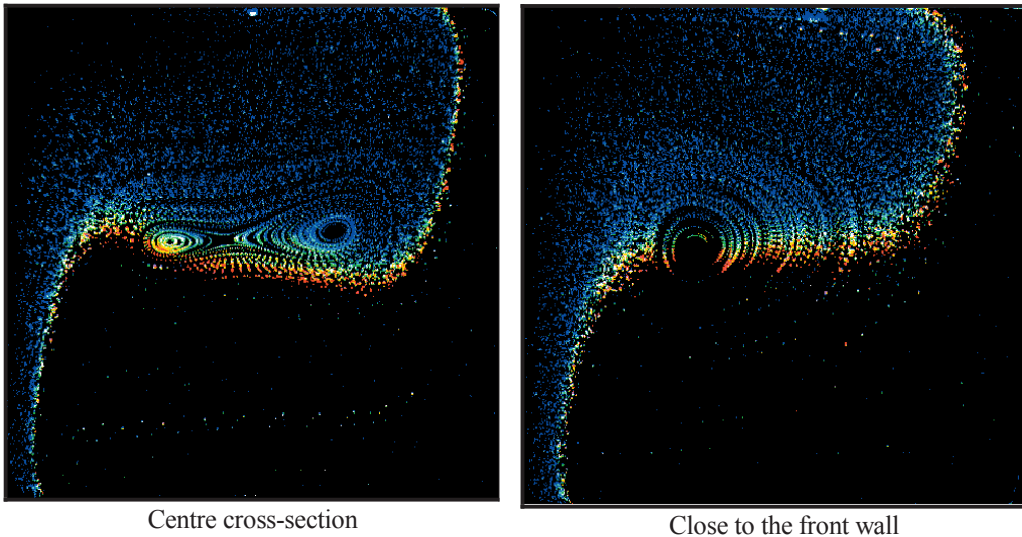


Figure 4. Multiexposed photographs of liquid crystal tracers in the convective flow in the differentially heated cubic cavity; the centre plane cross-section $z=0.5$ (left) and the front wall $z=0.95$ (right); $Pr=6300$, $Ra=8 \cdot 10^4$. Effect of thermal boundary conditions at side-walls - merging of the spiralling structure.

It is worth noting that numerical simulation using simple adiabatic *TBC* for the sidewalls, is generally in agreement with the velocity and temperature fields measured at the symmetry plane. This agreement deteriorates progressively as the front or back wall is approached (the nominally adiabatic, vertical walls of the cavity). Both the isotherms and the flow structure differ from those predicted by simulation (Hiller et al. 1990). The temperature field at side walls is characterized by larger horizontal gradients to non-adiabatic conditions existing there. For single convective cell system (low Rayleigh number), the axis becomes shifted towards one of the isothermal walls. The straight inner spiral arising in a numerical model for an adiabatic *TBC*, in reality, has its ends curved towards the hot wall. For the two-cell system, only one spiral initially reaches the front and back wall (Fig. 4). The two-cell flow structure forms characteristic “cats eyes” in the symmetry plane, and apparently merge midway between the centre and side walls. Several numerical investigations have explored this phenomenon. It appears that the shape and location of the merging region, as well as the direction and pitch of the inner spirals are extremely sensitive to *TBC* at all

non-isothermal walls. As a result the estimation of the proper *TBC* for the given experiment becomes a non-trivial task, especially for the two-cell system.

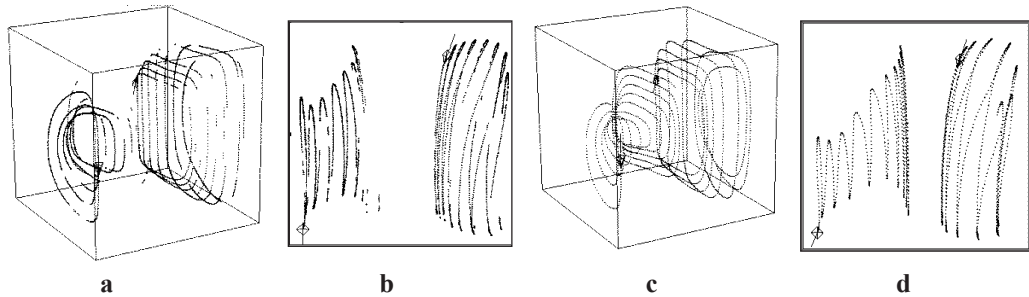


Figure 5. Particle tracks: a, b - measured, c, d - calculated using *TBC* from experiment; $Ra=4 \cdot 10^4$, $Pr=1180$. Isometric and top views of the cavity.

The process of defining an explicitly measured temperature distribution for all four non-isothermal walls replaced the trial-and-error method first used to fit the *TBC* (Hiller et al. 1992, Leonardi et al. 1999). Figure 5 shows a comparison between observed particle tracks and streamlines calculated with the experimentally defined wall temperatures. The direction and the pitch of the calculated spirals correlate well with those measured. The improvement indicated the need to modify the numerical model, i.e. the necessity for the 3-*D* modelling of heat transport through, and along, non-isothermal walls.

Particle accumulation and segregation in recirculating flow. The experimental investigation of the particle tracks usually helps us to determine whether an observed flow, is the same as one predicted by numerical simulation. New problems may also arise when particles are carried by flow. A physical particle has a finite size, mass and buoyancy. Hence, the residual hydrodynamic and gravitational forces acting on the particles may effect their distribution within the flow. Such redistribution of inclusions is also an important issue for purity in the quality of multi component melts during solidification. The experiment performed for simple convective flow in a differentially heated cavity demonstrates how apparently neutral particles aggregated after sufficient time. This occurs as a result of the cumulative effects of the periodic hydrodynamic interactions. Figure 6 shows the distribution of particles in the cavity after 100 hours and two weeks. The flow was initially uniformly seeded with an almost neutrally buoyant population of relatively large (0.35mm) particles. The recirculating convective flow field combined with the settling velocity traps most of particles in some flow regions, causing the rest of the cavity to become particle free. After about 100 hours one can identify a large ring of accumulated particles and a smaller, inner, ring structure. After two weeks almost all particles were confined to a small orbit on the left (warmer) side of the cavity.

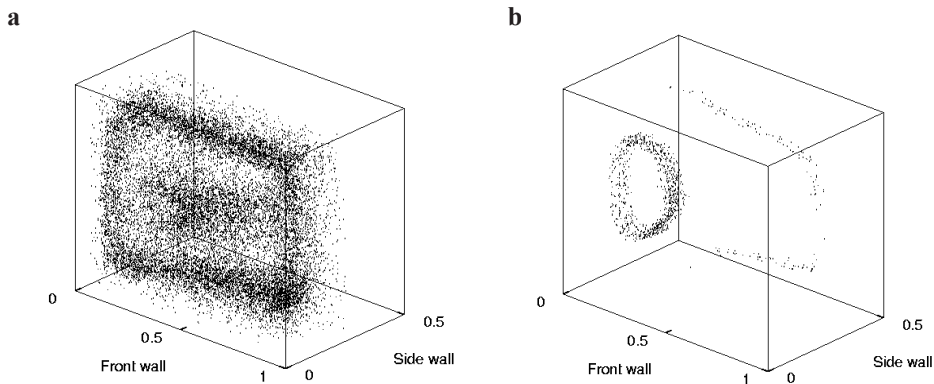


Figure 6. Isometric view of observed distribution of particles in a differentially heated cubic cavity after 100h (a) and two weeks (b); $Ra=10^5$. Only the front half of the cubic cavity is displayed.

Visualization of supercooling. Most of the investigations involving solidification assume isothermal conditions at the phase change boundary and temperatures above freezing point for the liquid phase. It is, however, well known that usually supercooling of the fluid usually precedes the phase change. Water of standard purity will normally, for example, supercool to about -5°C or -7°C before ice nucleation appears. It may retard the solidification process significantly. Freezing of the supercooled water results furthermore in the formation of a dendritic ice structure, which modifies the heat flux from the cooling wall. Thus, a better understanding of the role of supercooling in the solidification process seems necessary. The accurate modelling of supercooling is a non-trivial task. Supercooling depends on the purity of the fluid, concentration of the nucleation sites, the cooling rate, and sometimes even the cooling history. The theoretical prediction of the nucleation parameters is highly inaccurate. It is also not easy to extract quantitative information on the basis of empirical data only.

Our experiments with freezing water indicated that, in most cases, distilled water cools to about -7°C before phase change begins. The supercooled layer of liquid appears at the cold wall in the lid-cooled cavity. Its presence modifies the onset of convection. After cooling the lid for about 60s, the first ice layer, approximately 1mm thick, is observed. It propagates abruptly across the lid wall surface with a horizontal growth rate of approximately 40mm/s, several orders of magnitude faster than the subsequent thickening of the ice layer. In the differentially heated cavity, the observed effects of supercooling were even more dramatic, qualitatively changing the onset of freezing. In the cavity filled with warm water of 10°C , sudden cooling of the side wall to -10°C generated an instantaneous counter-clockwise vortex and an upward convection of the supercooled fluid. Figure 7 shows the supercooling using particle tracking. Colour images of liquid crystal tracers clearly indicate the presence of supercooled water along the wall (comp. Fig. 13a). During the first 40 to 60s, this supercooled water plum can cover a third of the upper surface before sudden freezing occurs. Within the next 10-15s, clockwise convective melting of excessive ice at the lid restores the regular plane propagation of the ice front. It would seem that supercooling changes

the initial circulation inside the cavity. The resulting heat transfer differs from that occurring in the standard situation. The initial ice layer also has a milky dendritic structure due to the supercooling.

Thermal conductivity of this non-homogeneous layer deviates from that of the pure solidus. Neither supercooling nor imperfections on the ice block were present in the numerical model. These may be the reasons for the difficulties encountered in achieving agreement between numerical and experimental data (Kowalewski & Rebow 1999, Banaszek et al. 1999).

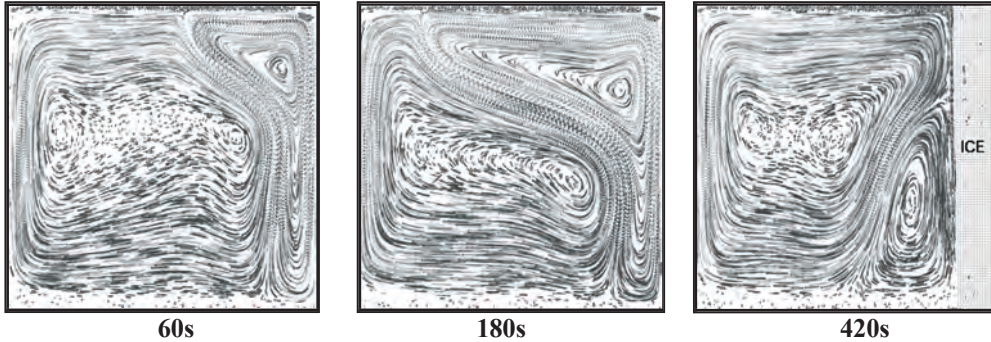


Figure 7. Supercooling of water freezing in differentially heated cubic cavity: $T_c = -10^\circ\text{C}$, $T_h = 10^\circ\text{C}$. Particle tracks by superposition of 20 images in the computer memory; Freezing experiment starts from developed convection.

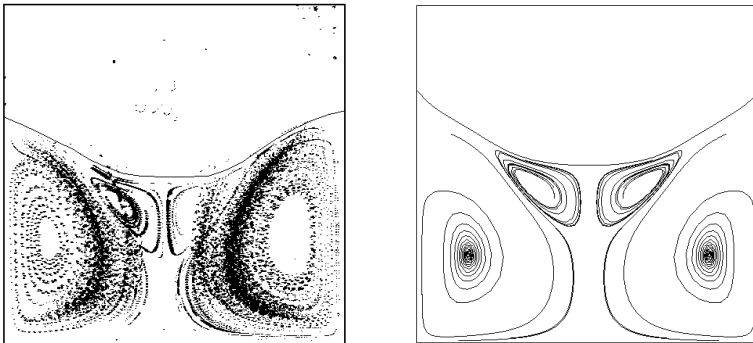


Figure 8. Natural convection beneath the ice surface. Particle tracks observed (left) and calculated (right) at the vertical centre plane. Lid-cooled cavity, $T_h = 20^\circ\text{C}$, $T_c = -10^\circ\text{C}$.

Particle tracks under the ice crystal. A comparison of the measured and predicted ice-water interface and the associated flow structures in the lid cooled cubic cavity can be viewed in Figure 8. A primary cell carries hot fluid up the wall to the ice interface, resulting in the recession of the outer edges of this interface. The water in the centre of the cavity then flows down. Just below the ice, in the centre of the cavity, small counter-rotating secondary flows are established due to the extreme density of the water around this region. This recirculation region plays an important role in limiting heat transfer through the thermal boundary layer at the ice surface. It is noteworthy that such a small region is practically invisible, in both the experimental and numerical velocity

fields. Only experimentally observed particle tracks allowed discovery of this density anomaly effects, which was confirmed afterwards by numerical tracks (Abegg et al. 1994).

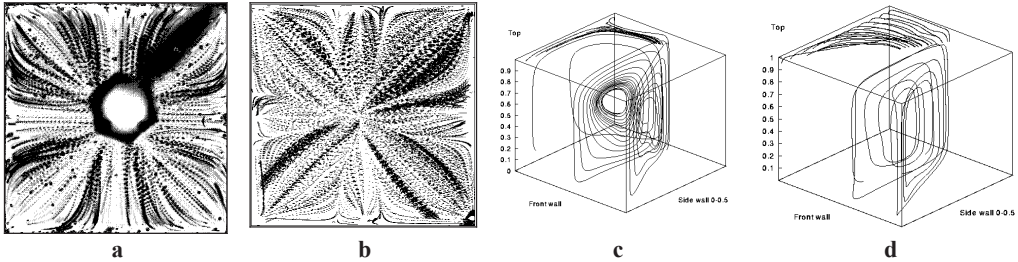


Figure 9. Lid cooled cavity, effect of *TBC* at side walls on pattern selection. (a, b) – particle tracking, top view underneath the lid; (c, d) - isometric view for numerical tracks. High conducting glass walls correspond to cases (a, c), low conducting Plexiglas walls to (b, d).

Flow pattern selection for a lid-cooled cavity. Flow visualization performed in a lid-cooled cavity using particle tracking shows the existence of a complex spiralling structure transporting fluid up along the side walls and down in a central cold plume along the cavity axis (Abegg et al. 1994). For walls of high heat conductivity (glass), eight symmetric cells formed in the flow. For Plexiglas walls, additional small regions of recirculation appeared separating the main cells. Although the computational results obtained for idealized, *1-D TBC* confirmed the eight-fold symmetry of the temperature and flow fields observed experimentally, their orientation was different (Abegg et al. 1994). Moreover, the isotherms were evidently shifted to higher values. Serious discrepancies in the temperature distribution at the horizontal cross-section were observed.

The heat flux was modified step-wise, over several simulations for the *1-D TBC* model to give better agreement with the measured temperature profiles. It was found that such agreement could be obtained by assuming nearly twice as much heat flux through the sidewalls as the nominal value calculated from the physical characteristics of the sidewalls (Leonardi et al 1999). This suggests that the heat flux along the sidewalls, neglected in the simple *1-D TBC* model, effectively increases the heat transfer from the surrounding medium. The difference between the observed and calculated flow patterns remained even after such seemingly arbitrary modification of the *TBC*. The calculated streamlines, starting in the diagonal symmetry plane, consequently spiralled in the *opposite direction* of that observed in experiments. *TBC* could not be properly modelled using an *1-D* of heat flux, especially, for 8mm thick Plexiglas walls. Physically it is indeed possible for a flow pattern with an opposite sense to develop one that spirals inwards at the central plane and outwards at the diagonal plane. Only a slight modification of the *TBC* therefore modifies the flow pattern and can be observed by replacing sidewalls of low conductivity Plexiglas with thin glass (Leonardi et al. 1999).

Numerical simulations performed of both cases, using the *3-D* model for wall heat conductivity, corroborated the *TBC* triggering mechanism for the flow pattern. The inclusion of sidewalls in the computational domain along with solving the coupled fluid-solid heat conduction problem improved the agreement with the observed flow pattern. The observed temperature distribution as well as its symmetry were fully recoverable from the numerical results. It was only as a result of

the use of *both* the experimental and numerical methods that the underlying fine mechanisms of the thermal flow were fully understood (Fig. 9).

3.2 Temperature visualization

Flow pattern selection for lid-cooled cavity. Liquid crystal tracers were used to investigate the temperature field beneath the lid for a cubic cavity. Both the temperature field and the star-like grooving of the ice surface indicate the eight-fold symmetry of the flow. Colour variation of TLC-seeded flow images taken directly under the lid (Fig. 10a,b) indicate a disparity in flow structure by differences observed in temperature pattern for low conducting Plexiglas sidewalls (Fig. 10a) and for well conducting glass walls (Fig. 10b). It appears that only a slight change of thermal boundary conditions at the sidewalls can modify the flow pattern.

An interesting example of the temperature pattern observed in the cylindrical cavity is shown in Fig. 10c. Despite the cylindrical symmetry, azimuthal flow structures appear, dividing the flow domain into regular sequence of 16-18 radially spiralling cells. This phenomenon was recently confirmed by numerical simulations (Gelgat et al. 1999). Experimental evidence of this flow symmetry-breaking was only possible with the help of TLC visualisation methods. These structures remain while the phase change is taking place. Characteristic star-like grooves in the ice surface growing at the lid follow the temperature field.

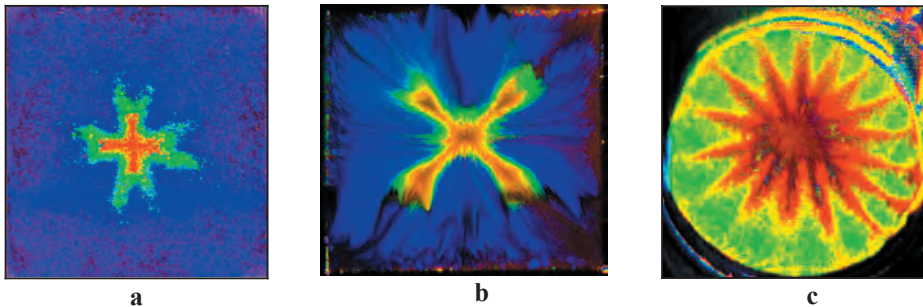


Figure 10. Natural convection in the lid cooled cavities. Temperature distribution recorded with help of TLC directly under the cooled top wall. Effect of the walls properties on the flow structure visible in the temperature fields: (a) - Plexiglas walls, (b) - glass walls, (c) - cylindrical glass cavity

Temperature distribution in lid cooled cylinder, comparing DSPI and TLC. Flow visualisation performed in lid-cooled cubic cavity shows a central cold jet along the cavity axis. Figures 11 displays temperature distribution obtained by tomographic reconstruction from DSPI images (Fig. 11b), and using thermochromic liquid crystals (Fig. 11c) (Soeller 1994).

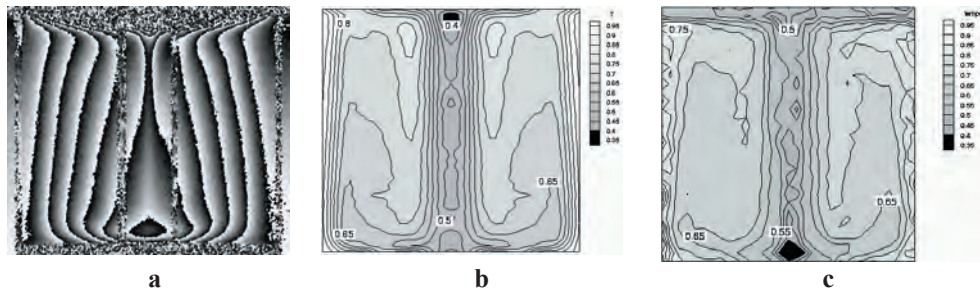


Figure 11. Temperature evaluation for lid cooled cubic cavity in vertical cross-section; (a) – DSPI speckle image for phase evaluation, (b) – DSPI evaluated temperature field, (c) – TLC evaluated temperature field.

“Hot-spots” visualization. The experimental model of the mould filling process was investigated. The experimental data were collected to create a reference database for comparison with numerical results. The method of simultaneous measurement of the flow and temperature fields using liquid crystal tracers has been successfully applied to collect transient information on the flow (Kowalewski et al. 2001). We consider forced convection in a rectangular, inclined box filled with viscous liquid. The cavity has square cross-section 38mm x 38mm and is 113mm high. The two sidewalls are made from 7.5mm tick Plexiglas. The other two isothermal sidewalls are made of copper. They are kept at low temperature T_c . Two Plexiglas plates located inside cavity are simulating shape complexity of a mould. They form three flow cavities connected only by 5mm high slits between the upper rim of the plates and the cold wall above. The cavity inclination angle α varied from 12° - 45° . The hot fluid of initial temperature T_h is forced to the cavity through a 13mm circular opening made in the bottom wall. Both forced convection and residual natural convection within the cavity are responsible for the heat transfer through the cold sidewalls.

Glycerol is used as the working fluid for its well known physical properties and very strong variation of viscosity with temperature. For the temperature range used ($T_c=10^\circ\text{C}$, $T_h=50^\circ\text{C}$) the fluid viscosity changes its value almost twenty times dramatically altering a flow pattern at the cold walls. The heat flux to the side cold walls is responsible for creation of the tick, viscous layer, retarding the main flow. It diminishes convective heat flux from the inner regions of the cavity. The cooling at some spots of fluid trapped in recirculation zones is delayed, leaving the “hot spots” (Fig. 12). In these places a slow conductive cooling and volumetric shrinkage of fluid can generate void bubbles, a common plague of any industrial casting. The observed interactions of free surface flow with the obstacles create an additional challenging problem for numerical simulations (Michalek & Kowalewski 2003).



Figure 12. TLC temperature visualization (left) and evaluated isotherms (right) observed just after closing the inlet; inclination of the cavity 26° . Blue colour (dark regions) indicates higher temperature.

Supercooling, temperature visualization

Supercooling of water visualized with classical tracers (Fig. 7) can be quantitatively evaluated using thermochromic liquid crystals. It can be seen (Fig. 13a) that before freezing starts, water at temperature below null rise up covering large part of the top wall. The degree of supercooling of about -7°C can be evaluated by dominant dark-red colour of the liquid crystal tracers in the rising plum.

Infrared Thermography. Freezing of water in differentially heated cubic cavity was investigated. Discrepancies between numerical and observed results forced us to verify Thermal Boundary Conditions imposed on the “passive”, non-isothermal sidewalls of the cavity. To control heat flux through these walls, measurement of both internal and external temperature fields at these walls becomes necessary. Such a possibility is offered by combined application of Infrared and TLCs based Thermography. Temperature fields obtained by IRT at external walls, and internal temperature maps from PIV & T measurements enrich our description of the physical experiment allowing better verification of numerical models (Wisniewski et al. 1998). Fig. 13b displays in false colours temperature distribution measured at the external front wall of the cavity. Temperature measured with accuracy equal to 0.3°C . The system used in our experimental studies consists of a low wavelength Agema Thermovision 900 LW infrared scanner. It uses a Mercury Cadmium Telluride (MCD) detector with liquid nitrogen cooling. The spectral band covered is from 8 to $12\ \mu\text{m}$, with some residual response outside this range. This spectral response results in low noise level measurements at room temperature. Nominal sensitivity of the scanner is equal to 0.08°C at 30°C .

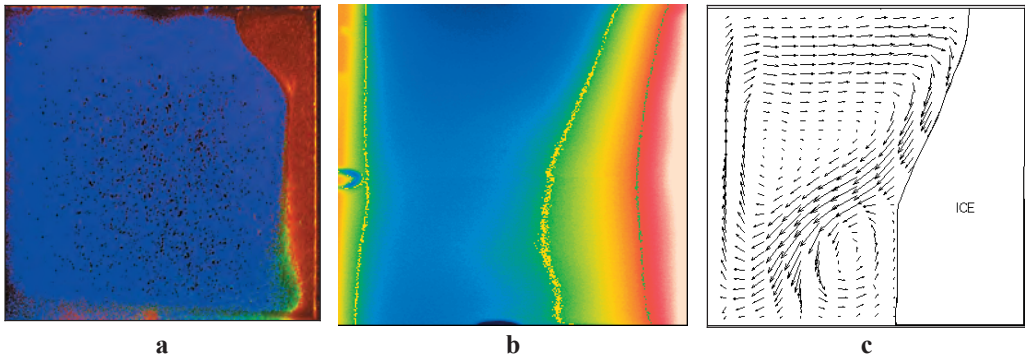


Figure 13. An example of combined application of liquid crystals and infrared thermography, and particle image velocimetry. Freezing of water in differentially heated cubical cavity ($T_c=-10^\circ\text{C}$, $T_h=10^\circ\text{C}$); (a) – initial supercooling, liquid crystal tracers show cold plum of water at temperature about -7°C (red colour); (b) - infrared temperature evaluation at the external front wall made of Plexiglas; (c) – velocity field measured by particle image velocimetry at the centre cross-section

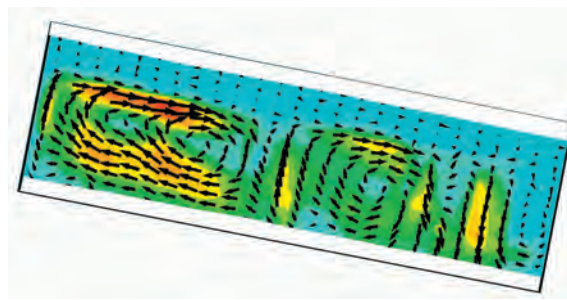


Figure 14: Water freezing in the mould model after its filling is accomplished. Ice layer is formed at both isothermal walls. Velocity vectors and contours of the velocity magnitude evaluated by PIV method. $T_c=-7^\circ\text{C}$, $T_h=9^\circ\text{C}$

3.3 Particle Image Velocimetry

Particle Image Velocimetry is applied to investigate flow field of water freezing in a differentially heated cubic box. The natural convection of water in the vicinity of the freezing point differs significantly from the well-known patterns of the benchmark solutions. The competing effects of positive and negative buoyancy forces result in a flow with two distinct circulations (Fig. 13c). There is a "normal" clockwise circulation, where the water density decreases with temperature (upper-left cavity region) and an "abnormal" convection with the opposite density variation and counter-clockwise rotation (lower-right region). At the upper part of the cold wall, the two circulations collide, intensifying the heat transfer and effectively decreasing the interface growth. Below, the abnormal circulation limits the convective heat transfer from the hot wall, separating it from the freezing front. Hence, the phase front is only initially flat. As time passes it deforms strongly, getting a characteristic "belly" at its lower part.

The experimental model of the mould filling process was investigated for inclined, simple rectangular cavity. The solidification process of water, the working fluid, is observed at both isothermal walls. Initially, almost uniformly and parallel to the wall, a layer of solid builds at both walls. However, as time progresses, the remaining effects of natural convection start to modify the heat transfer, resulting in a faster solidification at lower parts and an increase of asymmetry between upper and lower wall. The whole process depends on the inclination angle of the cavity. Figure 13 shows the experimental result obtained for water freezing in the cavity tilted at 11° . Initial water temperature was $+9^\circ\text{C}$, the isothermal walls temperature -7°C .

4 Laboratory benchmarks for solidification problems

Since numerical simulations in fluid dynamics reached certain level of maturity an increased attention is directed to define methodology of estimating errors and uncertainties of generated solutions. The problem of verification and validation of solutions became urgent for industrial applications, where costly prototypes have to be constructed on the basis of numerical predictions only. Sources of errors and uncertainties in results from simulations can be divided into two distinct sources: numerical modelling and physical modelling. Uncertainties and errors of numerical models can be again divided into several categories, where main are due to simplifications and approximations of mathematical problems (e.g. all discretization), and errors produced by numerical procedure. Uncertainties and errors of physical modelling are due to assumption and approximations made to describe physical reality. Formulating any problem we have to limit its mathematical description to certain domain, select more important parameters and neglect apparently less important. The only possibility to find out what does it mean is to perform experimental validation of the certain approach, comparing generated results with experimental data coming from a properly designed and evaluated experiment. The second part of the above sentence elucidates already next problem. How to find criteria for selecting an appropriate experiment? There are very limited experimental possibilities to deliver complete, transient description of velocity, temperature and concentration fields for industrial problems. It is not only because of not sufficiently developed of experimental tools, but also due to inaccurate or unknown physical properties of materials used, particularly by extreme thermal conditions, in presence of chemical reactions (e.g. oxidation, solubility) or at non-equilibrium states (e.g. supercooling). Hence, taking into account that it is very difficult to create profound experimental database for problems involving industrial scales and materials, small-scale experiments using model materials are used. Of course, such approach gives possibility to validate only part of the numerical model. When laboratory models are used there are serious differences in the scale of the problem, hence flow dynamics is usually different. Even more serious differences are in material properties. So-called *analog* fluids, simulating freezing of metals differ two or three orders of magnitude in Prandtl number, representing just opposite range of heat transfer properties. Therefore, single positive validation result, particularly using laboratory experiments, is a necessary but not sufficient condition to accomplish validation procedure, and several different tests have to be performed. In the following we give short review of few solidification experiments, which can be found in the literature together with three simple configurations we proposed as benchmarks for testing solidification problems.

4.1 Selection of the solidifying media and examples

Solidification of metals. Convection pattern in molten metals are difficult to determine experimentally, especially for buoyancy-driven flows. High melting temperature for most of the metals additionally complicates collection of data in the laboratory. Therefore, experiments performed with metals concern mainly measurements of temperature using thermocouples, and phase front location using X-rays or similar technique. Physical properties of some metals used in the laboratory experiments are collected in Table 4.1. The unique property of metals, impossible to model using other liquids, is high thermal conductivity, which leads to very low Prandtl number.

Perhaps one of most frequently cited paper concerning experimental investigation of metal solidification is that by Gau and Viskanta (1986). They used Gallium, low melting temperature metal to diminish experimental problems. Gallium has relatively well known physical properties; it is also technologically important material. The Prandtl number is 0.02. Experimental data were collected for 88.8mm x 63.5mm rectangular cavity with a free surface and differentially heated walls. Transient solidification and melting was investigated by collecting temperature distribution at the centreline with 26 thermocouples. The most valuable information collected are measurements of the liquid/solid interface at pre-selected time steps during melting. The pour-out and the probing method were used to examine and measure the shape of the interface. Hence, for each time the experiment was repeated. Despite its simplicity, experiment of Gau and Viskanta defined still useful experimental benchmark for validating simulation of melting metals. Desire for more detailed information, like temperature and a velocity field is obvious.

Table 4.1. Physical properties for typical metals used to simulate industrial solidification problems

| | Al | Sn | Ga |
|----------------------------------------------------------------|-----------------------|---------------------|----------------------|
| density, ρ [(kg m ⁻³)] | 2700 | 7280 | 6090 |
| specific heat, c [J kg ⁻¹ K ⁻¹] | 903 | 220 | 400 |
| thermal conductivity, k [W m ⁻¹ K ⁻¹] | 237 | 67 | 33.5 |
| thermal expansion, β [K ⁻¹] | $23 \cdot 10^{-5}$ | $27 \cdot 10^{-5}$ | $12 \cdot 10^{-5}$ |
| melting temperature, [°C] | 660 | 231 | 29.8 |
| kinematic viscosity, ν [m ² s ⁻¹] | 0.55×10^{-6} | $0.3 \cdot 10^{-6}$ | 3.1×10^{-6} |
| Prandtl number, Pr | $0.5 \cdot 10^{-2}$ | $1.5 \cdot 10^{-2}$ | $2 \cdot 10^{-2}$ |

Müller et al. (1984) have performed experiments with Gallium and Gallium doped with Antimony (GaSb) in vertical Bridgman configuration. Measurements of temperature were performed using thermocouples, microphotographs of crystals has been used to analyse perturbations of the interface due to the temperature oscillations. Collected data for Gallium are difficult to use for validation numerical simulation, but the paper shows analogical experiment performed for high Prandtl number fluid (water). It gives direction how to bypass experimental difficulties and collect flow pattern information using analog fluid.

An experimental benchmark test for “real life” problem was given by Sirrell et al. at the 7th Conference on Modelling of Casting (1995). The test consisted of a simple plate connected to a narrow and tall filling system. Characteristic dimensions of the plate were 200mm length, 100mm height, and 15mm depth. It was connected to a 410mm tall filling sprue. The geometry was filled

gravitationally with pure liquid aluminium. The real time X-ray radiographic unit was used to visualize the flow of liquid aluminium in the mould. The radiographic images were recorded at 50Hz on a videotape. Seven thermocouples were arranged in the mould to measure transient temperature variation. The whole filling process took about 2s, hence high speed turbulent flow was expected in the sprue. Two parameters were compared with nine numerical simulations: history of the interface and cooling rate traced by thermocouples. It appeared that despite very careful verification of thermophysical data used, and having all details of the mould geometry, it was difficult to find single code offering good agreement. Most of the codes had problems with modelling the interface instabilities. Also freezing times were not always in agreement. It is worth to note that proposed benchmark offered only global description of the process. Detailed temperature and velocity fields of the fluid were unknown, and couldn't be compared. Such comparison, if available, would be perhaps very helpful for identifications parts of the particular code that failed to simulate investigated phenomena.

Solidification of binary metal alloy. In most alloy solidification processes, a two-phase (mushy) zone forms. The zone is composed of solid dendrites and interdendritic liquid. The mushy zone separates solidified and melted regions strongly modifying heat and mass transfer through the interface. Because dendritic zone is permeable, flow may occur in the mushy zone, as well as in the melt. Concentration gradients within the zone generate solutal convection modifying flow at the interface. Complex coupling of the melt flow and the mushy zone flow is responsible for macrosegregation of alloy components, formation of voids, entrapment of inclusions and development of residual stresses. Numerical simulations of these processes are based on several crucial simplifications. Their validation appears imperative but difficult to perform. Experimental investigations of this complex processes flow are very limited.

Perhaps most comprehensive experiment was performed by Prescott et al. (1994). They provided details of the temperature and microstructure measurements for Pb-Sn alloy solidifying in an axisymmetric cell. The mould was suspended concentrically within the cooling jacket kept at 286K. The centrally located heater had temperature 578K. Dimensions of the cell were: inner radius 15.9mm, outer radius 63.5mm and height 150mm. Six sets of radially located thermocouples, immersed at three different depths were used to monitor temperature during solidification. Post-experiment measurements were made to determine the concentration of Pb by taking samples of material from several holes drilled in the mould. Metallographic analysis of specimens taken from experimental ingots was performed to provide information regarding characteristics of the mushy zone. Measurements were used to validate authors' numerical simulations. The cooling rates obtained from the temperature probes were critically analysed to conclude presence of a strong convection flow across dendritic structures, which is probably responsible for their fracturing and detachment. Detached, free-floating crystals could not be expected in the numerical model. Detailed analysis of temperature data recorded during solidification allowed for concluding about microsegregation pattern, indirectly confirming numerical predictions. Photographs of an ingot sections were used to analyse macrosegregation pattern and to estimate the permeability coefficient for the numerical simulations. The experiment gave evidence of thermosolutal convection, however indirectly as there were no flow dynamics measurements possible. It is worth noting, that even these limited experimental data gave evidence of undercooling, recalescence (heating

upon solidification), and solid particles transport. All these effects could not be predicted by numerical model.

Solidification of analog alloy models. Solutal and thermosolutal buoyancy forces play an important role in solidification process, giving rise to large-scale convection pattern. The resulting transport is termed *double-diffusive* convection. The phase change process is strongly influenced by a small-scale convective motion of the interdendritic liquid. The dendritic structure is described as porous media with some estimated permeability coefficient. Solidification process strongly depends on the complex interaction of the large-scale double-diffusive convection and filtration motion through the mushy zone. Numerical modelling of these flows depends on many unknown factors that can be only validated through experimental data. Experiments with metal alloys are not able to provide details on the mould flow. Hence, a variety of double-diffusive flows has been studied during solidification of optically transparent fluids, which freeze dendritically. These organic or aqueous solutions are known as *analog* alloys.

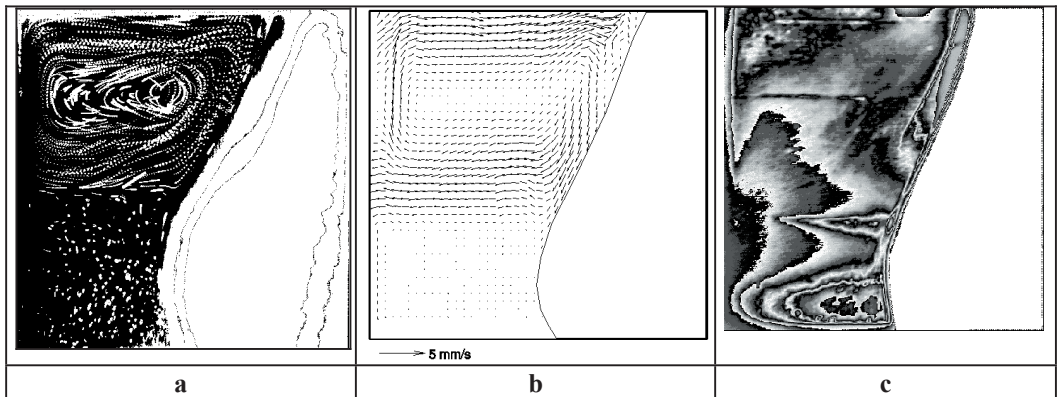


Figure 14. Solidification of NaCl aqueous solution: tracers (a), velocity field (b) and Schlieren image (c) (Kowalewski et al. 1998, Banaszek et al., IPPT 2000)

Figure 14 shows double-diffusive convection pattern during solidification of aqueous solution of NaCl in differentially heated cavity. Ice layer grows from the right sidewall. Salt rejected from the ice enriches boundary layer along the phase boundary. It induces solutal convection of denser liquid, which interacts with bulk thermal convection in the cavity. Flow stratification, which occurs along the bottom layer, is well visible in the velocity field. As a result of heating from the left wall, the second layer of fluid enriched with salt forms beneath the bottom layer. It is well visible in the schlieren image of the same flow (Fig. 4.2c). The solutal stratification may remain stable during main part of the solidification process. When the gap between hot wall and phase front decreases, the layer formed along the bottom extends vertically and becomes virtually stagnant.

Solidification of binary systems has been investigated for $\text{NH}_4\text{Cl}-\text{H}_2\text{O}$ solutions by Chang et al (1998). The schlieren images made for different salt concentrations demonstrate evolution of multi-layer system for hypoeutectic composition to double layered system with strong stratification

for hypereutectic compositions, with wave – like instability. It confirms previous observations reported by Beckerman and Viskanta (1988) for the same solution.

Water for its well-known properties, optical transparency, low melting temperature and simple handling is a best choice for laboratory experiments. The only problem, which can also be seen as a challenging advantage, is its anomaly of the density behaviour close to the freezing point. Beside water there are several, so-called phase-change-materials (PCMs) investigated intensively in the past as candidates for the energy storage. Some of them, like polyethylene glycol and n-octadecan, hexadecane, are used also for solidification in laboratory models. Another transparent organic liquid, believed to be a good analog for crystal growth problems is succinonitrile (SCN). Main physical properties of two typical *analog* fluids are collected in Table 4.2 and compared with water.

Table 4.2 Physical properties at melting point for materials used to simulate industrial solidification problems

| | Water | Succinonitrile SCN | Polyethylene glycol PEG 900 | Hexadecane |
|--------------------------------------------------------------|-----------------------|----------------------|-----------------------------|---------------------|
| density, ρ [(kg m ⁻³)] | 999 | 985 | 1100 | 792 |
| Specific heat, c [J kg ⁻¹ K ⁻¹] | 4217,8 | 2000 | 2260 | 2236 |
| thermal cond., k [W m ⁻¹ K ⁻¹] | 0.552 | 0.223 | 0.188 | 0.18 |
| thermal expansion, β [K ⁻¹] | $-0.07 \cdot 10^{-3}$ | $0.81 \cdot 10^{-3}$ | $0.76 \cdot 10^{-3}$ | $0.9 \cdot 10^{-3}$ |
| melting temperature, [°C] | 0 | 55 | 34 | 18 |
| kinematic viscosity, ν [m ² s ⁻¹] | $1.8 \cdot 10^{-6}$ | $2.6 \cdot 10^{-6}$ | $9 \cdot 10^{-5}$ | $3 \cdot 10^{-6}$ |
| Prandtl number, Pr | 13 | 23 | 1188 | 45 |

Selection of organic materials for investigations allows also to simulate behaviour of alloys. Frequently used in the laboratories *analog* alloy is succinonitrile with 0.2% wt acetone. This material is transparent and its solidification morphology resembles solidification of metals. It is used by Noël et al. (1997, 2000) for optical investigations of transient solidification process in vertical, cylindrical crucible. Details about interface structure, propagation of the instabilities were observed optically and detailed reported. However, despite transparency of the media, only information about the interface shape is given. It is perhaps not sufficient for detailed code validation.

Very detailed experimental study of SCN solidification in a horizontal Bridgman apparatus was reported by H. de Groh III (1994). The apparatus consists of a transparent glass ampoule with square cross-section and dimensions 6mm x 1500mm observed through the microscope. Melting is achieved by moving the heating-cooling jackets along the ampoule filled with pure SCN or SCN alloy. This experiment has been defined as an experimental benchmark at CHT'01 conference (Advances in Computational Heat Transfer, Palm Cove 2001). Experimental data available for the validation exercises consists of detailed description of the temperature history measured by thermocouples at five points on the external wall, location and shape of the interface, growth rate and flow visualization with seed particles. It is interesting to note that there was no response to this particular benchmark.

4.2 Proposed laboratory benchmark configurations

During last ten years several laboratory experiments were performed by our group to develop and improve methods of collecting quantitative data on velocity and temperature of convective motion accompanying solidification. With water as a flow media and thermochromic liquid crystals as tracers it is possible to collect transient information on temperature and velocity fields within several cross-sections of the flow. Also position and shape of the interface are retrieved from the images. The typical experimental setup we use for the flow measurements consists of a convection box, a halogen tube lamp, the 3-chip CCD colour camera and the 32-bit frame grabber. The flow field is illuminated with a 2mm thin sheet of white light from a specially constructed halogen lamp tube and observed in the perpendicular direction. It can be replaced with a Xenon flash lamp, if the flow velocity is high. The 24-bit true colour images, typically of 768x564 pixels, are acquired with a personal computer. Using PCI-bus RGB frame grabber (AM-STD ITI) the setup permits us to acquire into computer memory in real time a long sequence of true-colour images. Recording of the transient flow patterns and temperature fields is performed periodically. Typically every 10-300s, short series of images are acquired and stored on the hard disk of the computer for later evaluation. The computer controls the system of three stepping motors, switching of the light source and also records the readings from control thermocouples and the thermostats. Using three stepping motors two different configurations can be automatically arranged. First configuration, with a vertical light sheet directed by the mirror and the camera observing flow through the front wall is used to analyse flow in vertical planes. The second configuration, with a horizontal light sheet and the camera observing flow from the top through the mirror, allows to acquire horizontal cross-sections of the flow. The computer-controlled system allows for acquiring images of several cross-sections, fully automatically within several seconds. Hence, due to relatively slow variations of the flow structures, transient recording of the main three-dimensional flow features is possible.

In the experiments described below we consider natural convection of water freezing in a small cubic or rectangular cavities. A typical internal dimension of the investigated flow domain is 38mm for the cube. Either two opposite walls or one top wall are made of metal and assumed to be isothermal. Other walls are nominally insulators of finite thermal diffusivity. They are made out of 6 and 8mm thick Plexiglas or 2mm glass. The thermal conductivity of the "passive walls" seems to play an important role in the development of fine flow structures and the effect of their thickness and conductivity was investigated in different experiments.

Thermal properties of water vary with temperature. However, our numerical tests indicated (Leonardi et al. 1999) that it is appropriated to assume fluid heat capacity, thermal conductivity and viscosity constant. The values used in the numerical simulations are respectively:

$$\begin{aligned}c_1 &= 4.202 \text{kJ/kgK} \\k_1 &= 0.56 \text{W/mK} \\v &= 1.79 \cdot 10^{-6} \text{Ns/m}^2\end{aligned}$$

The fluid density varies with temperature according to the given polynomial function:

$$\rho_l = 999.840281167108 + 0.0673268037314653 \cdot t - 0.00894484552601798 \cdot t^2 + 8.78462866500416 \cdot 10^{-5} \cdot t^3 - 6.62139792627547 \cdot 10^{-7} \cdot t^4,$$

where the temperature t is given in degrees Celsius.

The thermophysical properties of ice we assume to be constant and equal: $\rho_s = 916.8\text{kg/m}^3$ for the density, $k_s = 2.26\text{W/mK}$ for the thermal conductivity, and $c_s = 2.116\text{kJ/kgK}$ for the heat capacity. The latent heat of freezing water is equal $L_f = 335\text{kJ/kg}$. The thermal conductivity, heat capacity and density of the Plexiglas used were measured. When solving the energy equation for the side walls, the values of 0.195W/mK for the thermal conductivity, and $1.19 \cdot 10^{-7}\text{m}^2/\text{s}$ for the thermal diffusivity were used. The heat transfer coefficient h used for modelling the convective heat flux from the external fluid was taken to be $20\text{W/m}^2\text{K}$ in case of a forced air flow outside investigated cavity, and $1000\text{W/m}^2\text{K}$ for the forced convection in water bath surrounding the cavity. Data were collected for about 3000s of the freezing process.

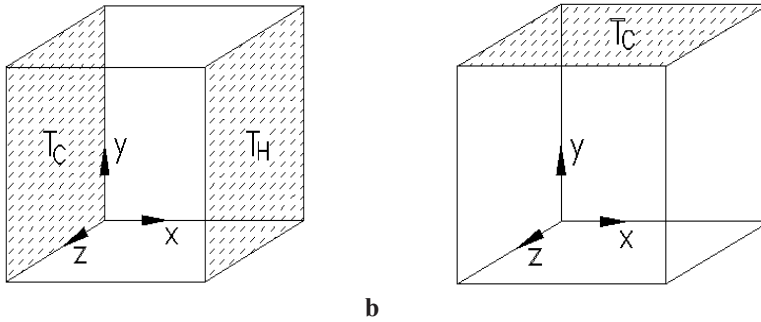


Figure 15. (a) - benchmark 1: differentially heated cavity, cube with two metal walls and four Plexiglas walls surrounded by air; (b) – benchmark 2: lid cooled cavity immersed in water bath, cube with the metal lid and with five Plexiglas walls; cavity is surrounded by an external water bath.

Benchmark problem 1, directional freezing in a differentially heated cavity: We consider convective flow in a box filled with distilled water (Fig. 15a). The flow takes place in a container with an aspect ratio of one, its two opposite vertical walls are assumed isothermal. Internal dimension of the box is 38mm. One of the vertical walls is held at temperature $T_c = -10^\circ\text{C}$. It is below the freezing temperature of water, hence the solidification takes place on this wall. The opposite vertical wall is held at temperature $T_h = 10^\circ\text{C}$. The isothermal walls are made of aluminium. The other four walls have low thermal conductivity, they are made of 6mm tick Plexiglas. The cavity is surrounded by a laminar stream of air at temperature $T_{\text{ext}} = 25^\circ\text{C}$. For transient processes uncertainty of the initial conditions may create difficulties in matching experimental and numerical results. Hence, to improve our definition of the initial condition, we start freezing after the steady convection pattern is established in the cavity. This initial flow state corresponds to natural convection without phase change in the differentially heated cavity, with the temperature of the cold wall set to $T_c = 0^\circ\text{C}$. The freezing experiment starts, when at time $t=0$, the cold wall temperature suddenly drops from null to $T_c = -10^\circ\text{C}$. In the numerical runs, the solution obtained for steady state natural convection was used as the initial flow and temperature fields to start the freezing calculations. The heat transfer coefficient h used for modelling the convective heat flux from the external fluid is taken to be $20\text{W/m}^2\text{K}$ for the forced air flow. Data are collected for about 3000s of the freezing process (about 30% volume is frozen). Below we give few examples of the data obtained.

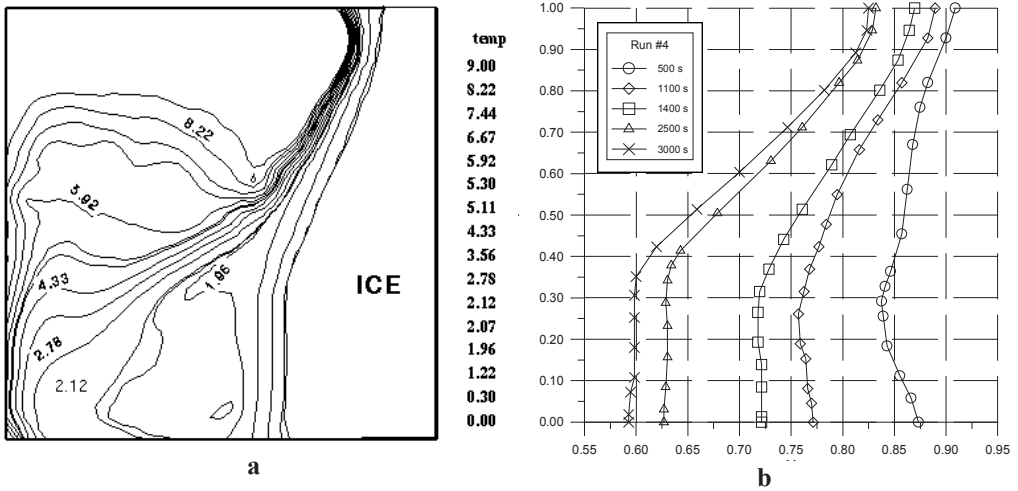


Figure 16. Freezing of water in differentially heated cube shaped cavity with four Plexiglas walls after 3000s. Left hot wall $T_h=10^{\circ}\text{C}$, right cold wall $T_c=-10^{\circ}\text{C}$; (a) - evaluated temperature distribution, (b) - phase front position. Compare also Fig. 12 showing evaluate velocity field and external wall temperature.

Figures 12 and 16 show examples of images showing behaviour of natural convection of water in the vicinity of the freezing point. It shows an interesting feature, two counter-rotating convection patterns, typical for the configuration with differentially heated walls. It is mainly due to the strongly non-linear temperature dependence of the density function with the extreme at 4°C . The competing effects of positive and negative buoyancy force result in a flow with two distinct circulations. There is a "normal" clockwise circulation, where the water density decreases with temperature (upper-left cavity region) and an "abnormal" convection with the opposite density variation and counter-clockwise rotation (lower-right region). At the upper part of the cold wall the two circulations collide with each other, intensifying the heat transfer and effectively decreasing the interface growth. Below, the convective heat transfer from the hot wall is limited by the abnormal circulation, separating it from the freezing front. Hence, the phase front is only initially flat. As time passes it deforms strongly, getting a characteristic "belly" at its lower part. High temperature and velocity gradients in the region of two colliding circulation patterns create challenging condition for numerical modelling. Our experimentation and numerical simulations have shown the enormous sensitivity of the flow structure and the freezing front to relatively small changes of the hot wall temperature or thermal boundary conditions at the passive walls (Leonardi et al. 1999). The simulations confirmed most of the details of the flow for the initial time steps (below 500s). However, as time proceeds the ice growth rate delays significantly in comparison to the numerical predictions (Kowalewski & Rebow 1999, Giangi et al. 1999, 2000).

Benchmark problem 2, vertical Bridgman freezing problem in lid cooled cavity: We consider convective flow in a cube filled with distilled water. The top wall of the container is assumed isothermal and is held at temperature $T_c=-10^{\circ}\text{C}$. It is below the freezing temperature of water and ice crystal growths from the lid down into the cavity. Internal dimension of the box is 38mm, the

five side walls are made of Plexiglas. The wall thickness is 8mm. The Plexiglas cube is immersed in an external water bath of temperature $+20^{\circ}\text{C}$ (see Fig. 15b). We assumed that for a forced convection in the bath the heat transfer coefficient is $h = 1000\text{W}/\text{m}^2\text{K}$. All other details are similar as in the benchmark 1. The isothermal metal lid has temperature -10°C , when freezing is investigated. But as described above, we start the freezing experiment (and simulations) after natural convection is developed, initially setting the top wall temperature to 0°C at the beginning.

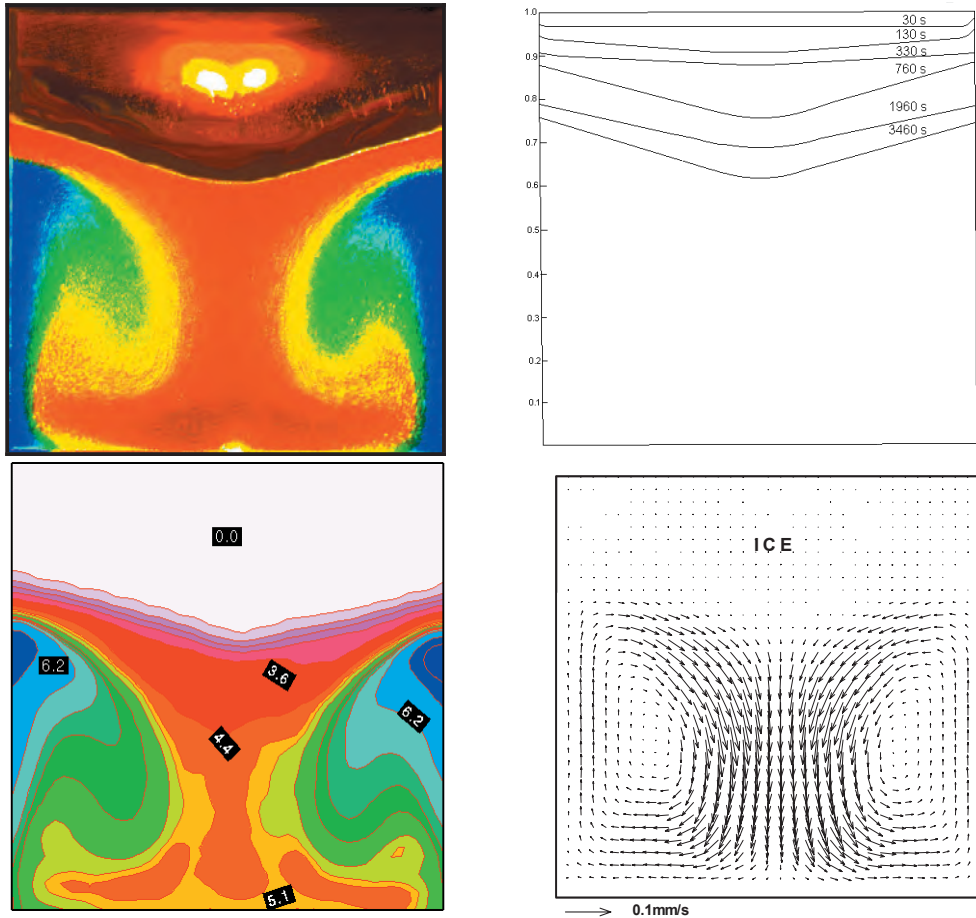


Figure 17. Freezing of water in the lid-cooled cavity. Top line: liquid crystals visualization (left), phase front profiles for selected time steps (right). Bottom line: evaluated temperature field (left) and velocity field (right) for natural convection in the centre plane at 3600s. Top wall temperature $T_c = -10^{\circ}\text{C}$, external bath temperature $T_h = 20^{\circ}\text{C}$; $Ra = 1.5 \cdot 10^6$, $Pr = 13.3$

The data on interface position, velocity and temperature fields are collected periodically during about 3600s of the freezing process. After this time approximately 35% of the cavity volume is frozen. Figure 17 shows examples of the data acquired. Strong deformation of the initially flat ice

front is well visible. The crystal has conical shape due to the recirculating flow in the cavity. The cold liquid penetrates along the cavity axis into the bottom, warms up and returns along the side walls. Detailed observations indicated presence of eight-fold symmetry of the recirculating flow field, it is reproduced in the star-like grooving present at the ice surface. These was confirmed by performed numerical simulations. However, like in the previous case, the simulated growth rate of ice seriously deviates form the observed for longer time steps (Kowalewski & Cybulski 1996, 1997).

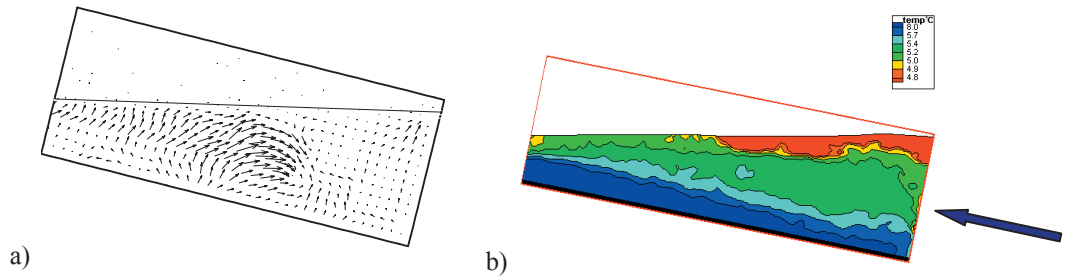
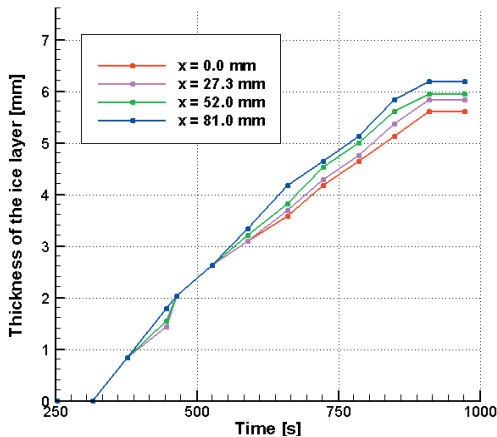


Figure 18. Flow observed in mould filling model at $t=20s$. Water at initial temperature T_H is forced through the 13mm opening in the bottom wall (arrow). It freezes at two side metal walls kept at temperature T_C . The remaining four walls (top, bottom, front and back) are made of Plexiglas. (a) - PIT evaluated velocity field; (b) - PIT evaluated isotherms. Inclination $\alpha = 78.6^\circ$, flow rate $4.6 \cdot 10^{-6} m^3/s$

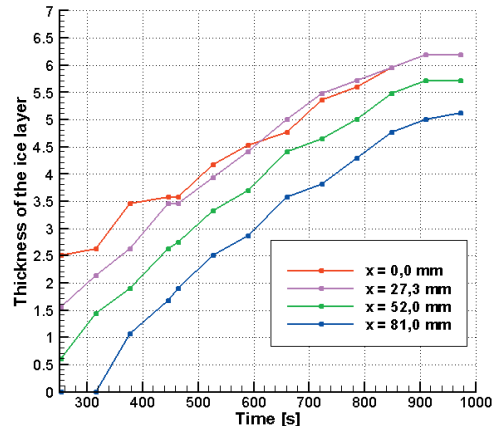
Benchmark problem 3, mould filling with freezing in inclined rectangular cavity: The experiments are performed in a small (113mm x 38mm x 38mm) rectangular cavity made of 7.5mm Plexiglas. The cavity is inclined, with the inclination angle from vertical $\alpha=78.6^\circ$. The two opposite side-walls made of copper are assumed to be isothermal. They are kept at low temperature $T_c = -10^\circ C$. Water is used as a working fluid. The fluid of initial temperature $T_h = 25^\circ C$ is forced to the cavity through a 13mm circular opening made in the bottom wall. The flow rate is $4.6 \cdot 10^{-6} m^3/s$. Both forced convection and residual natural convection within the cavity are responsible for the heat transfer through the cold side-walls (Kowalewski et al. 2001, Cybulski et al. 2002). Due to the inclination, liquid film slips down through the opening gap and the cavity is filled (Fig. 18). After the whole cavity is completely filled the flow is immediately interrupted and fluid trapped in the cavity starts to cool down. Stable thermal stratification develops along the isothermal walls, and cooling is mainly due to the conduction. Observed residual natural convection is very weak, especially close to the freezing point. During filling process and afterwards the freezing front propagates at both isothermal walls. Initially the growth rate of ice at the lower wall is faster than at the upper one (Fig.19). But after about 4 minutes this difference vanishes completely and the uniform growth of the ice layer is observed for both walls. Transient parameters measured in the experiment are: position and shape of the free surface, position and shape of the freezing front, fluid temperature and velocity fields for centre cross-section, temperature measured by 12 thermocouples at the isothermal walls (3 points each wall), at the side wall (three points) and at the inlet and outlet. Despite of using 20mm thick copper blocks with coolant pumped through by two heavy duty thermostats, temperature of the “isothermal” walls is not constant during the filling process. It drops down about $3^\circ C$ during filling process. It nearly completely recovers after

filling process is finished. Hence, the transient temperature data for the metal walls must be used to simulate properly the cooling process.

Using several commercial codes to simulate this experiment we came to the conclusion that even this very simple experimental model of the mould is difficult enough to create challenging problem. Several details are difficult to reproduce numerically, like formation of the recirculating zones during filling process. Also growth rate of the solid phase differs quite seriously. It gave us indication of some weak points present in commercial codes used.



Thickness of the ice layer at the upper wall



Thickness of the ice layer at the lower wall

Figure 19. Experimental data for the ice thickness variation in time during filling and freezing process measured at 4 intervals from the bottom wall (inlet).

5. Conclusions

Convection with phase change can be analysed by variety of techniques. Some of them we mentioned in above. Assuming that the main message of the experiment is to deliver reliable and dense data about several flow parameters, full field and volumetric methods are favourable selection. Here we have in mind such methods like particle image velocimetry and thermometry (liquid crystal tracers), infrared thermography, all sets for tomographic reconstruction of temperature and concentration fields, and still useful interferometry with its holographic extension. However, trying to deliver experimental data for industrial configuration most of the modern optical methods must be excluded. Remaining methods are less accurate and still far from mature status (like industrial tomography). Hence, we have to solve typical dilemma. Is it better to test industrial code using inaccurate industrial experiment or is it better to replace materials used and try to simulate both experimentally and numerically selected physical features, typical for the industrial problem. Not all such features can be present, at least simultaneously. But if we encounter problems with simulating such simplified cases, can we have confidence in large-scale simulations with industrial materials?

Finally we do hope that experimental analysis of the simplified flow configuration, supported by numerical tests, allows for better identification of parameters playing crucial role in the specific

flow problem. It offers unique possibility to perform sensitivity analysis of the problem, delivering information about tolerance span for the accuracy of defining material properties, in description of boundary conditions and flow geometry. Such analysis is essential for planning large scale industrial configuration but also very useful for determining code validation experimental procedure.

Acknowledgements. This is summary of the work which author was fortunate to share with his colleagues and students, first at the Max-Planck-Institut Goettingen and presently at his home institution. In particular contributions of W. Hiller, St. Koch, Ch. Soeller, A. Cybulski and M. Rebow are grateful acknowledged. A part of the present research was supported by Polish Scientific Committee (KBN Grant No. 8T09A00820).

References

- Abegg, C., de Vahl Davis, G., Hiller, W.J., Koch, St., Kowalewski, T.A., Leonardi, E., Yeoh, G.H. (1994). Experimental and numerical study of three-dimensional natural convection and freezing in water. *Proc. of 10th Int. Heat Transfer Conf.*, ed. G.F. Hewitt, Ichem 4:1-6.
- Andres, N., Arroyo, M.P., Quantilla, M. (1999). Interferometric techniques for measuring flow velocity fields. *Machine Graphics & Vision* 8: 625-636.
- Banaszek, J., Jaluria, Y., Kowalewski, T.A., Rebow, M. (1999). Semi-implicit FEM analysis of natural convection in freezing water. *Num. Heat Transfer Part A*: 36:449-472.
- Banaszek, J., Kowalewski, T. A., Furmanski, P., Rebow, M., Cybulski, A., Wisniewski, T.S. (2000). Natural convection with phase change in one-component and binary systems. *IPPT Reports* 3/2000, IPPT PAN Warszawa.
- Bartels-Lehnhoff, H.H.(1991). *Erfassung dreidimensionaler Bahnlinien und Geschwindigkeitsfelder mittels automatischer Bildverarbeitung*. Ph.D. Thesis in Mitteilungen aus dem MPI 101, Göttingen.
- Beckermann, C., Viskanta, R.(1989). Effect of solid subcooling on natural convection of a pure metal. *J. Heat Transfer (ASME)* 111: 416-424.
- Bovik, A. (2000). *Handbook of Image and Video Processing*. Academic Press, San Diego.
- Brito, D., Nataf, H.C., Cardin, Ph., Aubert, J., Masson, J.P.(2001). Ultrasonic Doppler velocimeter in liquid gallium. *Exp. in Fluids* 31:653-663.
- Carlomagno G.M. (1993). Heat transfer measurements by means of infrared thermography, in *Measurement Techniques*. VKI Lect. Series 1993-05, Rhode-Saint-Genese. 1-114.
- Chang, Y.J., Hsieh, Y.T., Chen, Y.M.(1998). Flow visualisation during a water freezing process by holographic interferometry. In *8th Int. Symp. on Flow Visualization*. 114.1-8.
- Cybulski A., Michałek T., T.A. Kowalewski, M. Kowalczyk, M. Sokolnicki (2002). Experimental and numerical simulation of mould filling process, *Proceedings of Int. Conference Heat 2002*, Baranow S. June 2002. 267-272.
- Dabiri, D., Gharib, M. (1991). Digital particle image thermometry: The method and implementation. *Exp. in Fluids* 97: 77-86.
- Emrich, R.J. (1981). *Methods of Experimental Physics*. Vol. 18 Fluid Dynamics. Academic Press, New York.
- Englemann, D., Garbe, Ch., Stöhr, M., Geißler, P., Hering, F., Jähne, B. (1988). Stereo particle tracking, in *Proc. 8th Int. Symp. Flow Visualization*. 240.1-8.
- Fomin, N.A. (1998). *Speckle Photography for Fluid Mechanics Measurements*. Springer Verlag, Berlin-Heidelberg-New York.

- Gau, C., Viskanta, R. (1986). Melting and solidification of a pure metal on a vertical wall. *J. Heat Transfer (ASME)* 108:174-181.
- Gelfgat, A.Yu, Bar-Yoseph, P.Z., Solan, A., Kowalewski T.A. (1999). An axisymmetry breaking instability of axially symmetric natural convection *Int. J. Trans. Phenomena* 1:173-190.
- Giangi, M., Kowalewski, T.A., Stella, F., Leonardi, E. (2000). Natural convection during ice formation: numerical simulation vs. experimental results. *Comp. Assisted Mech. and Eng. Scs.* 7: 321-342.
- Giangi, M., Stella, F., Kowalewski, T.A. (1999). Phase-change problems with free convection: fixed grid simulation. *Comp. & Vis. in Scs.* 2:123-130.
- Gobin, D., Le Quere, P. (2000). Melting from an isothermal vertical wall. Synthesis of numerical comparison exercise. *Comp. Assisted Mech. and Eng. Scs.* 7:289-306.
- Goldstein, R.J.(1983). Fluid Mechanics Measurements. Hemisphere, Pub. Corp., Washington.
- Grant, I., Thompson, B.J.(eds). (1994). *Selected Papers on Particle Image Velocimetry*. SPIE Milestone Series MS99, Optical Eng. Press, Bellingham.
- Groh III de, H.C. (1994). *Interface shape and convection during solidification and melting of succinonitrile*. NASA Tech. Memorandum 106487.
- Gui, L., Merzkirch, W. (1996). A method of tracking ensembles of particle images. *Exp. in Fluids* 21:465-468.
- Gui, L., Merzkirch, W. (2000). Comparative study of the MQD method and several correlation-based PIV evaluation algorithms. *Exp. in Fluids* 28:36-44.
- Hay, J.K., Hollingsworth, D.K. (1996). A comparison of trichromic systems for use in the calibration of polymer-dispersed thermochromic liquid crystals. *Exp. Thermal Fluid Scs*, 12:1-12
- Hiller, W., Kowalewski, T.A.(1987). Simultaneous measurement of the temperature and velocity fields in thermal convective flows. *In Flow Visualization IV*, Ed. Claude Veret, Hemisphere, Paris. 617-622.
- Hiller, W.J., Koch, St., Kowalewski, T.A. (1988). Simultane Erfassung von Temperatur- und Geschwindigkeitsfeldern in einer thermischen Konvektionsströmung mit ungekapselten Flüssigkristalltracern. *In: 2D-Meßtechnik DGLR-Workshop*, Markdorf, DGLR-Bericht 88-04, DGLR Bonn.31-39.
- Hiller, W.J., Koch, St., Kowalewski, T.A. (1989). Three-dimensional structures in laminar natural convection in a cube enclosure. *Exp. Therm. and Fluid Sci.* 2:34-44.
- Hiller, W.J., Koch, St., Kowalewski, T.A., de Vahl Davis, G., Behnia, M. (1990). Experimental and numerical investigation of natural convection in a cube with two heated side walls, *Proc.of IUTAM Symposium*, Cambridge UK, Aug. 13-18, 1989, (Edits. H.K. Moffat & A. Tsinober), CUP.717-726.
- Hiller, W.J., Koch, St., Kowalewski, T.A., Mitgau, P., Range, K. (1992). Visualization of 3-D natural convection. *Proceedings of The Sixth International Symposium on Flow Visualization*, Eds. Tanida Y. & Miyashiro H. Springer-Verlag. 674-678.
- Hiller, W.J., Koch, St., Kowalewski, T.A., Stella, F. (1993). Onset of natural convection in a cube. *Int. J. Heat Mass Transfer* 36:3251-3263.
- Ibrahim, S., Green, R.G., Evans, K., Dutton K.(2000). Flow visualisation using optical tomography. *In Proc. 9th Int. Symp. Flow Visualization*. 140.1-8.
- Incropera, F.P. (1997). Experimental methods for characterizing transport phenomena occurring during solidification of multi-constituent materials. In Proc. Exp. Heat Transfer, Fluid Mech. and Thermodynamics, Edizioni ETS. 1855-1865.
- Jähne, B.(1997). *Digital Image Processing*. Springer Verlag, Berlin-Heidelberg-New York.
- Koch, St. (1993). *Berührungslose Messung von Temperatur und Geschwindigkeit in freier Konvektion*, Ph.D. Thesis in Mitteilungen aus dem MPI 108, Göttingen.
- Kowalewski, T. A., Cybulski, A. (1997). Natural convection with phase change. *IPPT Reports* 8/97, IPPT PAN Warszawa .
- Kowalewski, T. A., Cybulski, A.(1996). Experimental and numerical investigations of natural convection in freezing water. *Int. Conf. on Heat Transfer with Change of Phase*, Kielce. In Mechanics 61/2:7-16.

- Kowalewski, T.A. (1998). Experimental validation of numerical codes in thermally driven flows. *In Advances in Computational Heat Transfer*, G. de Vahl Davis, E. Leonardi (eds), Begel House Inc., New York. 1-15.
- Kowalewski, T.A., Cybulski, A., Sobiecki, T. (2001). Experimental model for casting problems. *In Computational Methods and Experimental Measurements*, Eds. Y. V. Esteve, G.M. Carlomagno, C.A. Brebia, WIT Press, Southampton. 179-188.
- Kowalewski, T.A., Rebow, M. (1999). Freezing of water in the differentially heated cubic cavity. *Int. J. Comp. Fluid Dyn.* 11:193-210.
- Lehner, M., Mewes, D., Dingreiter, U., Tauscher, R. (1999). *Applied Optical Measurements*. Springer Verlag, Berlin-Heidelberg-New York.
- Leonardi, E., Kowalewski, T.A., Timchenko, V., de Vahl Davis, G. (1999). Effect of finite wall conductivity on flow structures in natural convection. *Proceedings of the International Conference on Computational Heat and Mass Transfer*, Cyprus, eds. A.A. Mohamad & I. Sezai, Eastern Mediterranean University Printinghouse. 182-188.
- Mayinger, F., Feldmann O. (2001). *Optical Measurements, Techniques and Applications*. Springer-Verlag, Berlin-Heidelberg-New York.
- McDonough, M.W., Faghri, A. (1994). Experimental and numerical analyses of the natural convection of water through its density maximum in a rectangular enclosure. *Int. J. Heat Mass Transfer* 37:783-801.
- Michalek, T., Kowalewski, T.A. (2003). Experimental model of mould filling flow. *In Eurotherm 69 Heat and Mass Transfer in Solid-Liquid Phase Change Processes*, eds.: B. Šarler, D. Gobin
- Mishima, K., Hibiki, T. (1996). Quantitative limits of thermal and fluid phenomena measurements using neutron attenuation characteristics of materials. *Exp. Thermal Fluid Scs.* 12:461-472.
- Mitgau, P.M., Hiller, W.J., Kowalewski, T.A. (1994). Verfolgung von Teilchen in einer dreidimensionalen Strömung. *ZAMM* 74(5):T394-396.
- Müller, G., Neumann, G., Weber, W. (1984). Natural convection in vertical bridgman configurations. *J. Crystal growth* 70:78-91.
- Noël, N., Jamgotchian, H., Billa, B. (1997). *In situ* and real-time observation of the formation and dynamics of a cellular interface in a succinonitrile-0.5%wt acetone alloy directionally solidified in a cylinder. *J. Crystal growth* 181:117-132.
- Noël, N., Zamkotsian, F., Jamgotchian, H., Billa, B. (2000). Optical device dedicated to the non-destructive observation and characterization of the solidification of bulk transparent alloy *in situ* and real time. *Meas. Sci. Technol.* 11:66-73.
- Park, H.G., Dabiri, D., Gharib, M. (2001). Digital particle image velocimetry/thermometry and application to the wake of a heated circular cylinder. *Exp. in Fluids* 30:327-338.
- Pham, A.H., Hua, Y., Gray, N.B. (1999). Eddy current tomography for metal solidification imaging. In 1st World Congress on Industrial Process Tomography, Buxton. 451-458.
- Plaskowski, A., Beck, M.S., Thorn, R., Dyakowski, T. (1994). *Imaging Industrial Flows*. IPP, Bristol and Philadelphia.
- Praisner, T.J., Sabatino, D.R., Smith, C.R. (2001). Simultaneously combined liquid crystal surface heat transfer and PIV flow-field measurements. *Exp. in Fluids* 300:1-10.
- Prescott, P.J., Incropera, F.P. (1994). Convection transport phenomena and microsegregation during solidification of a binary metal alloy: Part 1 & 2. *J. Heat Transfer (ASME)* 116:735-749.
- Prescott, P.J., Incropera, F.P. (1996). Convection heat and mass transfer in alloy solidification. *Adv. in Heat Transfer* 28:231-338.
- Quénot, G., Pakleza, J., Kowalewski, T.A. (1998). Particle Image Velocimetry with Optical Flow. *Exp. in Fluids* 25:177-189.

- Raffel, M., Willert, C., Kompenhans, J. (1998). *Particle Image Velocimetry*. Springer Verlag, Berlin-Heidelberg-New York.
- Rinkevichius, B.S. (1998). *Laser Diagnostics in Fluid Mechanics*. Begell House Inc., New York, Wallingford.
- Roache, P.J. (1997). Quantification of uncertainty in computational fluid dynamics. *Ann. Rev. Fluid Mech.* 29:123-160.
- Rucki Z., Szczepanik Z, Blogowska K. (2002). Measurements of the resistance filed in binary mixture with freezing (in Polish), *PW Prace Naukowe-Konferencje*, Conference XVIII Zjazd Termodyn., printed by Politechnika Warszawska, 22: 991-1000.
- Sabatino, D.R., Praisner, T.J., Smith, C.R. (2000). A high-accuracy calibration technique for thermo-chromic liquid crystal temperature measurements. *Exp. in Fluids* 28:497-505.
- Sielschott, H. (1997). Measurement of horizontal flow in a large scale furnace using acoustic vector tomography. *Flow Meas. and Instr.* 8:191-197.
- Sirrel, B., Holliday, M., Cambell, J. (1995). The benchmark test 1995. *In Proc. of the 7th Conference on Modelling of Casing, Welding and Advanced Solidification Process*, TMS Pub. 915-933.
- Soeller, C. (1994). *Untersuchung der Konvektionsströmung in von oben gekühlten Behältern mittels tomographischer Speckle-Interferometrie und digitaler Bildverarbeitung*. Dissertation, University of Göttingen.
- Straley, S.M.J. (1974). Physics of Liquid Crystals. *Review of Modern Physics* 46/4:617-704.
- Takeda, Y. (1999). Ultrasonic Doppler method for velocity profile measurement in fluid dynamics and fluid engineering. *Exp. in Fluids* 26:177-178.
- Van Buren, P.D., Viskanta, R. (1980). Interferometric measurement of heat transfer during melting from a vertical surface. *Int. J. Heat Mass Transfer* 23:568-571.
- Viskanta, R. (1988). Heat transfer during melting and solidification of metals. *J. Heat Transfer (ASME)* 110:1205-1219.
- Westerweel, J. (1993). *Digital Particle Image Velocimetry - Theory and Application*. Delft, Delft University Press.
- Westerweel, J., Dabiri, D., Gharib, M. (1997). The effect of a discrete window offset on the accuracy of cross-correlation analysis of digital PIV recordings. *Exp. in Fluids* 23:20-28.
- Xu, H., Fife, S., Andereck, C.D. (2002). Ultrasound thermal imaging (UTI) of convective opaque fluids. *Eurotherm Seminar 71 Proceedings* Reims (France), Oct. 28-30, 2002 (Edits. C. Padet & H. Burkhardt), University of Reims. 331-336.
- Yarin, A., Kowalewski, T.A., Hiller, W.J., Koch, St. (1996). Distribution of particles suspended in 3D laminar convection flow. *Physics of Fluids* 8:1130-1140.